MARGINAL MOMENT GENERATING FUNCTION BASED SUBOPTIMAL ADAPTIVE ANALYSIS FOR GENERALIZED-K FADING — A COMPOSITE MODEL FOR FADING CHANNELS

Dissertation Submitted in partial fulfillment of the degree of

Master of Technology

in

Electronics and Communication Engineering

Under the supervision of

PROF. GHANSHYAM SINGH

by

AAKANKSHA SHARMA

DEPARTMENT OF ELECTRONICS AND COMMUNICATION ENGINEERING

JAYPEE UNIVERSITY OF INFORMATION TECHNOLOGY

SOLAN – 173 215, INDIA

Roll No. 132009 **MAY-2015**

JAYPEE UNIVERSITY OF INFORMATION TECHNOLOGY
(Established by H.P. State Legislative vide Act No. 14 of 2002)
P.O. Waknaghat, Teh. Kandaghat, Distt. Solan - 173234 (H.P.) INDIA
Website: www.juit.ac.in
Phone No. (91) 01792-257999 (30 Lines)
Fax: +91-01792-245362

CERTIFICATE

This is to certify that the work entitled, "***Marginal moment generating function based suboptimal adaptive analysis for Generalized-K fading — a composite model for fading channels***" submitted by ***Aakanksha Sharma*** in partial fulfillment for the award of degree of ***Master of Technology*** **in** ***Electronics and Communication Engineering*****, Jaypee University of Information Technology, Solan**, has been carried out under my supervision. This work has not been submitted partially or wholly to any other University or Institute for the award of this or any other degree or diploma.

(Dr. G. Singh)

(Supervisor)

ABSTRACT

A novel scheme based on the communication among the distributed nodes has motivated the use of composite fading models because the distributed nodes experience different levels of multipath/small scale fading, shadowing and path loss. Most of the composite fading models consider multipath fading superimposed on lognormal shadowing distribution. However, the analysis using these composite fading models with complex integral form is not able to provide closed form expressions. Therefore, the composite fading model using Generalized-K distribution is provided in which the lognormal distribution is approximated by Gamma distribution in order to have simplified and closed-form expressions. Further, the analysis is provided using moment generating function (MGF) because of its advantage over simplification of the mathematical expressions as compared to that of the probability density function (PDF) based approach. The improvement over capacity performance of the communication system is provided by adapting the transmission rate, power and coding techniques of the transmitter in accordance to the channel state information (CSI). The channel capacity for suboptimal adaptation technique over the Generalized-K fading environment is presented. The analytical expression for channel capacity for truncated channel inversion with fixed rate (C_{TCIFR}) has been provided in terms of marginal moment generating function (MMGF) and its performance is evaluated over the Generalized-K faded environment. This MMGF based approach for the computation of channel capacity has been validated with the reported literature for channel capacity for channel inversion with fixed rate suboptimal adaptive technique.

Another part of dissertation concerns with the DAS with *N* number of distributed ports per cell. The composite fading model for DAS is provided with combined effect of path loss, shadowing and small scale fading. The distributed relay nodes (RN) have emerged as a technology for improved system capacity and cell edge coverage by exploiting the benefits of both macro-diversity as well as micro-diversity. The generalized analytical expressions are presented for the fixed and transparent relaying between the base station and the mobile station in presence of composite fading environment with single node relaying and multiple node relaying. The closed-form expressions for the outage

probability and the channel capacity analysis for a distributed antenna system (DAS) are provided using Gauss-Hermite quadrature approximation.

ACKNOWLEDGEMENT

I would like to extend my sincere gratitude towards my dissertation advisor, **Prof. Ghanshyam Singh**, for giving me an opportunity to be a part of his research work. His constant motivation and support made me to complete my work and I am indebted for his valuable advice both in technical and non technical matters.

I am also grateful to **Prof. T.S. Lamba**, Dean (Academic and Research) and **Prof. S.V. Bhooshan**, Head, Department of Electronics and Communication for their encouragement and illuminating discussion.

I would also like to thank Dr. Vivek K. Dwivedi and Dr. Raja Durai for their help and taking out time for answering my questions that made me to understand the concepts more precisely.

I am also grateful to the committee members, Dr. D.S. Saini, Dr. Shruti Jain and Mr. Munish Sood for their valuable comments and guidance that motivated me for improvement and to explore my potential.

I would like to thank all my friends (Himangi Sood, Bindu Bharti, Poonam Kango, Subhash Chandra Tiwari, Prabhat Thakur and Khushvinder Thakur) and my seniors (Shweta Pandit, Keerti Tiwari and Garima Bharti) for being there always to help me and to make the environment at Research lab worth for working.

Last but not the least; I would like to thank my parents and brother for their patience, support and showing confidence in me throughout my course. They have always stood there for me and were a constant source of inspiration whenever I felt low. Above all, praise is to God, the most gracious, without whose blessing my accomplishments would have never been possible.

Aakanksha Sharma

CONTENTS

LIST OF FIGURES

LIST OF PUBLICATIONS

[1] Aakanksha Sharma, V. K. Dwivedi and G. Singh, “Channel capacity with suboptimal adaptation technique over Generalized-K fading using marginal moment generating function”, IEEE/ACM Transactions on Networking, (Under Review), May 2015.

[2] Aakanksha Sharma and G. Singh, “Analysis of channel capacity and outage probability for distributed antenna system over composite fading channel”, Wireless Personal Communications, (Under Review), May 2015.

CHAPTER 1

AN OVERVIEW OF FADING CHANNEL MODELS IN DISTRIBUTED COMMUNICATION SYSTEMS

1.1 Introduction

1.1.1 Fading in wireless communication channel

Communication system basically consists of three basic elements, namely, 1) Transmitter, 2) Receiver and 3) Communication channel. Depending upon the type of communication channel (medium that connects the transmitter and the receiver), we have basically two main types of communication systems i.e., 1) Wire-line and 2) Wireless communication systems. Wireless communication systems have experienced exponential growth in the years and despite of their prominent application in present scenario, they pose certain major drawbacks such as the random variation in its impulse response and it's highly indeterministic characteristics. The wireless communication channel in contrast to the wire line channel is random and in-deterministic and therefore, its estimation is a difficult task [1]. The time variant characteristics of the wireless communication channel have lead to severe multipath and shadow fading. A precise mathematical model for the approximation of the wireless channel behavior is either unknown or too complex to be employed for communication system analysis. Methods to discover simpler approximation techniques have been investigated over the past years and thus, have lead to an immense scope of research in the field of estimation and modeling of wireless communication channel for more accurate analysis of the communication systems. The most frequently assumed model for digital communications channel is additive white Gaussian noise (AWGN) channel. However, AWGN is not an accurate model for the wireless channels and therefore a non Gaussian channel is provided, that is a fading channel. This section defines the basic phenomenon for fading and its types along with the various statistical models used for their simulation. Detailed description for the characteristics of fading is available in several standard books [2, 3].

The wireless channel is more prone to the losses introduced by noise, interference and obstructions, which provides time dependent variation to signal in an unpredictable manner. This random variation in signal strength, when combined at the receiver is termed as 'fading'. The electromagnetic wave propagation (through which signal propagates along the medium) consist of several mechanisms such as:

1. Reflection,
2. Diffraction, and
3. Scattering.

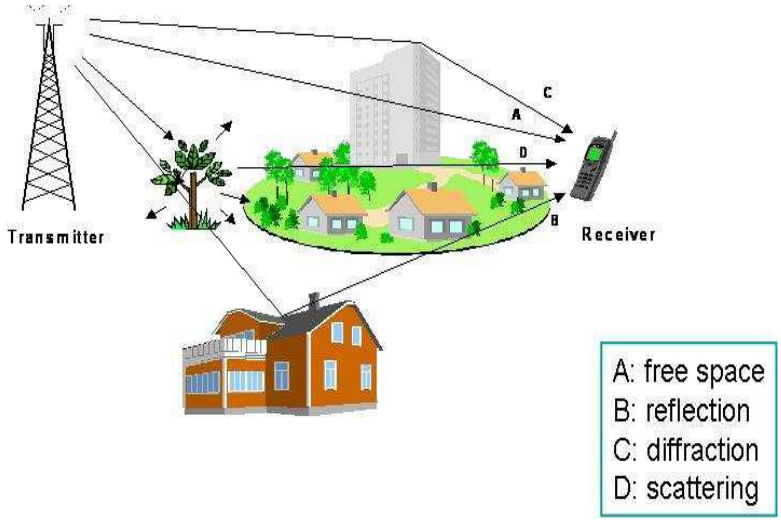

Fig.1.1 Physical mechanisms in wireless signal propagation [4]

The main mechanisms in electromagnetic wave propagation are shown in Fig.1.1 and are discussed in detail as:

Reflection: Reflections arise when the plane waves are incident upon a smooth surface with dimensions that are large enough as compared to the wavelength($D \gg \lambda$). In Fig.1.1, B represents the reflection mechanism. This phenomenon can be modeled by General Ray Tracing (GRT) model [2- 4].

Diffraction: These mechanisms arise when the wave is incident upon the dense scatterers with dimensions greater than the wavelength($D > \lambda$) and results into bending of wave across their sharp edges. It occurs according to Huygen's principle where secondary wavelets are produced due to presence of obstruction between transmitter and receiver

and these secondary wavelets propagates behind the obstruction resulting in low levels of signal power. In Fig.1.1, C shows the diffraction of a wave. Diffraction is most commonly modeled by the Fresnel knife-edge diffraction model [2- 4].

Scattering: Scattering occurs when the wave is incident upon the scatterers having rough surface and irregular shapes with dimensions approximately equal to that of the signal wavelength($D \approx \lambda$). It is modeled by using Radar cross section (RCS) model. In scattering, wave gets distributed along all the directions and is shown by D in Fig.1.1 [2-4].

The aforementioned mechanisms form the basis for random variation in received signal power over time or fading. Here, we have categorized fading on the basis of distance over which these variations occur as: 1) Large scale fading and 2) Small scale fading [2- 4].

Large scale fading is defined as the signal power attenuation or path loss due to motion over large areas or distances. It depends upon the scatterers present between the transmitter and receiver, position of receiver and the distance between the transmitter and receiver. The statistics of large scale fading provides the signal variation as a function of distance. Large scale fading generally consist of mean path loss variation and a log normally distributed variation termed as shadowing. Path loss usually refers to the signal power attenuation due to absorption by atmosphere and depends upon the distance between the transmitter and receiver. Whereas, shadowing results due to diffraction from the sharp edges of buildings or towers.

Small scale fading represents signal variations over a short distance i.e. approximately equal to that of signal wavelength. Small scale fading is also termed as multipath fading as multiple copies of same signal are received at the receiver antenna resulting due to various propagation mechanisms such as reflection, scattering and diffraction. The multiple copies add up together either constructively or destructively at the receiver antenna to generate the resultant received signal. The small scale variations are related to the channel impulse response. The mobile radio channel can be modeled as a linear time varying channel, where variations are with respect to time and distance.

Figure 1.2 shows the hierarchy for fading in wireless communication channel categorized mainly as large scale fading and small scale fading. We generally define power delay profile (PDP) for the analysis of multipath or small scale fading. Small scale fading can be further categorized on the basis of time dispersion parameters (TDP) and frequency dispersion parameters (FDP) as Flat or Frequency selective fading and Fast or Slow fading respectively. Detailed description for the mentioned categories of fading and the statistical models that are used for their approximation is provided in the next section [2, 3].

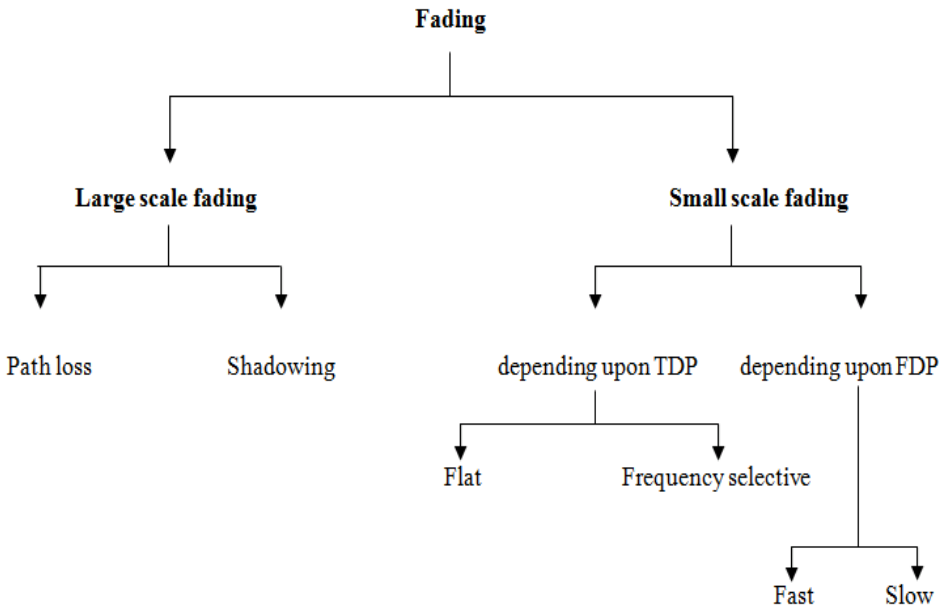

Fig.1.2. Hierarchy for fading in wireless communication channel.

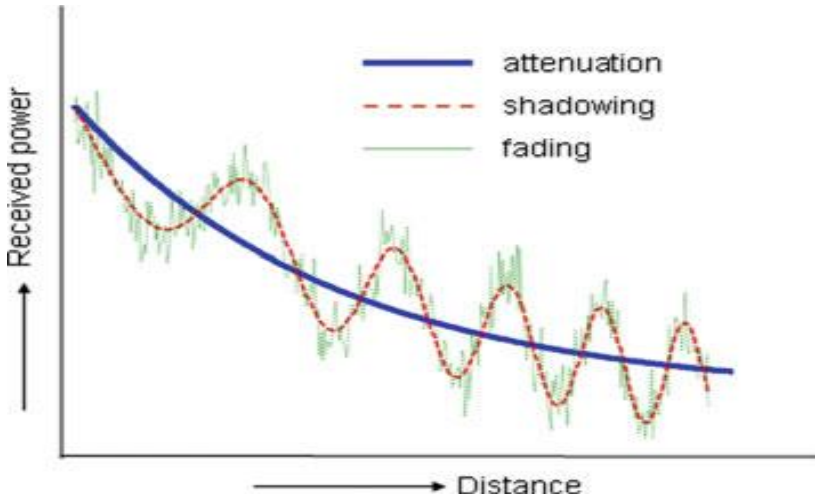

Fig.1.3. Received power variation for path loss, shadowing and multipath fading with respect to distance [5]

1.1.1.1 Path loss

The path loss is defined as the signal variation due to propagation of signal from transmitter to the receiver. It generally results due to power dissipation of transmitted signal and some propagating mechanisms such as absorption by the atmosphere and represents the signal power variation over large distances of the order of hundreds or thousands of meters. Path loss models assume a distance based variation i.e. the received power is a function of distance between the transmitter and receiver. Simplest path loss model corresponds to free space propagation model in which no obstructions are assumed to be present between the transmitter and the receiver and the signal propagates through a line of sight (LOS). The received signal power decay is given as a function of raised to some power of the distance between the transmitter and receiver. The received signal power is given by Friis free space equation as [2, 3]:

$$\mathrm{P_r}(d) = \frac{P_t G_t G_r \lambda^2}{(4\pi d)^2} \tag{1.1}$$

where, P_t is the transmitted power, $\mathrm{P_r}(d)$ is the received signal power, G_t and G_r is the transmitting antenna gain and receiving antenna gain respectively, λ is the signal wavelength and d is the distance between the transmitter and the receiver. The above equation shows that the received signal power decreases with the factor of square of distance between the transmitter and the receiver under free space propagation and is

directly proportional to the wavelength. Thus, for higher transmitting frequencies, the path loss is also high. Generalizing above equation for other propagating scenario we have

$$\mathrm{P_r}(d) = \frac{P_t G_t G_r \lambda^n}{(4\pi)^2\, d^n} \tag{1.2}$$

where, n is the path loss exponent and its value varies from 2 to 6; n = 2, 3-4 and 4-6 for free space, outdoor and indoor channels respectively [6, 7].

1.1.1.2 Shadowing

Shadowing results due to obstruction present in between the transmitter and the receiver which completely blocks the signal and therefore, a shadowed region is created which results into low received signal power at the receivers placed in the shadowed region. The main mechanism behind shadowing is diffraction at the sharp edges of obstructions which results into secondary wavelets. Shadowing results into received signal power variation within few meters of area or distance. Figure 1.4 shows the scenario for shadowing as

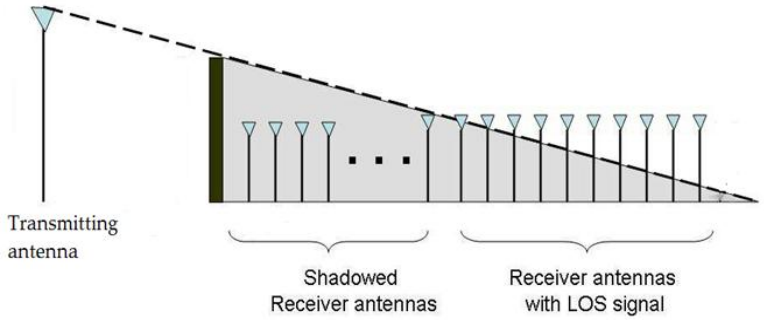

Fig.1.4. The shadowed region formed due to sharp edge of obstruction present between the transmitter and the receiver [4].

Shadowing is modeled by using lognormal distribution, where the log normally distributed random variable is $X = \frac{P_t}{P_r}$ and the logarithmic of this random variable follows normal distribution. P_t is the transmitted signal power and P_r is received signal power. The probability density function for log normal distribution is given as [2- 4]

$$P(X) = \frac{1}{x\sqrt{2\pi}\sigma} \exp\left(\frac{-(lnx - \mu)^2}{2\sigma^2}\right) \tag{1.3}$$

where, μ and σ represents the mean and standard deviation for lognormal distribution.

1.1.1.3 Small scale fading or multipath fading

Small scale fading represents signal variations over a short distance i.e. approximately to that of wavelength. Small scale fading is termed as multipath fading as multiple copies of same signal are received at the receiver antenna. The multiple copies due to delay, reflection, diffraction and/or scattering add up together either constructively or destructively at the receiver antenna to generate the resultant received signal with varying signal power. The small scale variations are related to the channel impulse response. The mobile radio channel can be modeled as a linear time varying channel, where variations are with respect to time and distance. Power delay profile (PDP) of the channel is obtained by the spatial average of square of the magnitude of the channel impulse response over a local area. Several measurements form an ensemble of PDP, where each represents the instantaneous channel state. Depending upon the various parameters of multipath channel, we can further categorize small scale fading. Time dispersion parameters of the multipath channel cause signal to have either flat or frequency selective fading. For flat fading, signal bandwidth is very much less than the flat fading channel bandwidth and therefore the flat fading channels are also known as narrowband channels. In this type of fading spectral characteristics are preserved but the strength of the signal varies with time. However, for frequency selective fading, the bandwidth of signal is greater than the channel bandwidth and therefore, frequency selective fading channels are also known as wideband channels. As time varies, the channel varies in gain and phase across the spectrum of the transmitted signal, resulting in time varying distortion in received signal. Frequency dispersion parameters basically defines the time varying nature and thus, depending on how rapidly the transmitted signal varies as compared to the rate of change of the channel, the fading is categorized as fast fading or slow fading. In fast fading channel, impulse response changes rapidly i.e. the coherence time of channel is smaller than the transmitted symbol period. In this type of fading signal is distorted due to frequency dispersion, which results due to Doppler spreading. It occurs for very low data rates. However, in slow fading channel, the channel impulse response varies at a much slower rate as compared to the transmitted signal i.e. the coherence time of channel is greater than the transmitted symbol period. The decision that whether the

signal is fast faded or slowly faded depends upon the velocity of mobile or velocity of objects in the channel. [2, 3]

The multipath formed in small scale fading can be modeled by using Rayleigh, Nakagami-q (Hoyt), Nakagami-n (Rician), Nakagami-m or Weibull distribution depending upon the type of fading scenario.

Rayleigh distribution

Multipath fading is modeled by using Rayleigh distribution when there is no direct LOS path that is in urban and suburban areas [8- 10]. The probability density function for channel fading amplitude is given as [11]

$$p_{\alpha}(\alpha) = \frac{2\alpha}{\Omega}\exp\left(\frac{-\alpha^2}{\Omega}\right) \quad , \qquad \alpha \geq 0 \tag{1.4}$$

where, α represents the fading amplitude and Ω represents the average value of the signal power. The instantaneous signal to noise ratio (SNR) follows the distribution given by

$$P_{\gamma}(\gamma) = \frac{1}{\bar{\gamma}}\ exp\left(\frac{-\gamma}{\bar{\gamma}}\right) \ , \qquad \gamma \geq 0 \tag{1.5}$$

where, γ is the instantaneous received SNR and $\bar{\gamma}$ is the average received SNR. Amount of fading (AF) or fading figure for Rayleigh fading is 1. This model is usually applicable for propagation of reflected and refracted path through troposphere and ionosphere and ship to ship links [12].

Nakagami-q or Hoyt distribution

This distribution is characterized by the signal fading parameter q $(0 \leq q \leq 1)$. The instantaneous SNR distribution is given as [13]

$$P_{\gamma}(\gamma) = \frac{1+q^2}{2q\bar{\gamma}}\ exp\left[\frac{-\left(1+q^2\right)^2\gamma}{4q^2\bar{\gamma}}\right] I_o\left(\frac{\left(1-q^4\right)\gamma}{4q^2\bar{\gamma}}\right) \ , \qquad \gamma \geq 0 \tag{1.6}$$

where, γ is the instantaneous SNR and $\bar{\gamma}$ is the average received SNR. $I_o(.)$ represents the zeroth order modified Bessel function of first kind [14, Eq. (8.445)]. The AF for Hoyt distribution is given as $\frac{2(1+q^4)}{(1+q^2)^2}$ and thus, its value varies from 1 (for $q = 1$ and represents

Rayleigh distribution) to 2 (for $q = 0$ and represents one sided Gaussian fading). Hoyt distribution is used to model satellite links with strong ionospheric scintillation [15]. Hoyt distribution and Rician distribution has been used to model two-state mobile satellite propagation channel [16].

Nakagami-n or Rician distribution

This distribution is used in the scenario with one strong LOS and many random weaker components and is used to model microcellular urban and suburban mobile channels and picocellular indoor environments [17]. The parameter n with values varying from 0 to ∞ is used to characterize this type of distribution with distribution of instantaneous SNR as [18]

$$P_\gamma(\gamma) = \frac{(1+n^2)e^{-n^2}}{\bar{\gamma}}\ exp\left[\frac{-(1+n^2)\gamma}{\bar{\gamma}}\right]\ I_o\left(2n\sqrt{\frac{(1+n^2)\gamma}{\bar{\gamma}}}\right)\ , \qquad \gamma \geq 0 \tag{1.7}$$

where, γ is the instantaneous SNR and $\bar{\gamma}$ is the average received SNR. $I_o(.)$ represents the zeroth order modified Bessel function of first kind [14, Eq. (8.445)]. AF is given as $\frac{1+2n^2}{(1+n^2)^2}$ and thus varying from 0 (for $n = \infty$ and represents no fading) to 1 (for $n = 0$ and represents Rayleigh distribution).

Nakagami-m distribution

This distribution is the most generalized case as it can be used to model all the aforementioned scenarios by varying the value of its parameter. The value of parameter m varies from 0.5 to ∞ with $m = 0.5,1, < 1\ and\ > 1$ representing one sided Gaussian, Rayleigh, Nakagami-q and Nakagami-n or Rician distribution respectively [19, Eq. (11)]. Instantaneous SNR is distributed as follows

$$P_\gamma(\gamma) = \frac{m^m \gamma^{m-1}}{\bar{\gamma}^m\ \Gamma(m)}\ exp\left(\frac{-m\gamma}{\bar{\gamma}}\right)\ , \qquad \gamma \geq 0 \tag{1.8}$$

where, γ is the instantaneous SNR and $\bar{\gamma}$ is the average received SNR. The AF for Nakagami-m is given as $\frac{1}{m}$ and thus varies from 0 (for $n = \infty$ and represents no fading) to 2 (for $n = 0$ and represents one sided Gaussian fading) [4, 5].

Weibull distribution

This type of distribution is generally used to model the random variable which is a non linear function of zero mean Gaussian distributed random variable [20]. The PDF of Weibull distribution is represented as [21]

$$P_R(r) = \frac{\alpha r^{\alpha-1}}{\Omega}\ exp\left(\frac{-r^{\alpha}}{\Omega}\right) \tag{1.9}$$

where, α is the parameter that determines the level of fading with $\alpha = 2$ and $\alpha = 1$ for Rayleigh fading channel and exponential distribution respectively [22]. Weibull distribution has been used to model indoor propagation environment [23]. Furthermore, channel modeling for narrow-band digital enhanced cordless telecommunications system at reference frequency of 1.89 GHz has been done by using Weibull distribution [24]. Weibull distribution is used to model multipath fading channel for outdoor communication [25].

The aforementioned statistical models independently model a single type of fading channel considering only one type of fading irrespective of the others and therefore will not give accurate approximation for wireless channel and thus performance analysis of wireless communication systems would not be reliable. Also, as we are moving to communication over distributed ports or nodes, the use of composite fading model comes into role as distributed nodes or ports experience different level of fading and shadowing. To have a better approximation of wireless channel we need to consider all categories of fading simultaneously which forms the basis for requirement of a composite model. In most of the cases for composite fading models, received power variation due to path loss is assumed to be identical and can be ignored while forming a composite model as distance between transmitter and receiver is assumed to be known always. Since we are heading towards the communication among distributed ports therefore we need to have the basic introduction for such type of system models.

1.1.2 Distributed Antenna System

Wireless communication has lead to an exponential growth over the decade. However, this increase in number of users has lead to limited wireless resources and thus transmission over large distance is not achievable with large transmission rate. Therefore, to have improvement over cell edge coverage, connectivity, capacity and spatial diversity gains, antennas are distributed throughout the cell which are connected to the base station (BS) and thus, reduces the distance of transmission for the mobile station (MS). Such type of antenna system is called distributed antenna system (DAS) in which communication between the transmitter and the receiver is achieved by the technique called relaying [26- 28]. The relaying techniques in distributed communication systems are classified as:

1. Transparent relaying or non regenerative relaying technique and
2. Regenerative relaying technique.

The transparent relaying does not modify the information or signal received or may allow simple amplification and/or phase rotations. It includes amplify and forward relaying, linear process and forward relaying and non-linear process and forward relaying. In contrast, the regenerative relaying technique as the name indicates, modify the received information or signal and thus require signaling mechanisms and complex operations. It includes decode and forward, estimate and forward and compress and forward relaying techniques [29-31]. Depending upon the flexibility of relay nodes, they can be classified as:

1. Fixed relay nodes and
2. Mobile relay nodes.

Fixed relay nodes comprises of fixed radio infrastructure and their movement is restricted. However, mobile relay nodes have flexible radio infrastructure [32, 33]. In between the BS and the MS, there can be single relay node or multiple relay nodes. The multiple relay nodes can be operated with multiple hops, where the nodes are connected in series and with dual hop, where the nodes are connected in parallel in order to have improvement over the path loss gain and diversity gain, respectively [29].

Figure 1.5 (a) and (b) shows the multiple relay nodes in series combination with multiple hop transmission and in parallel combination with dual hop transmission, respectively.

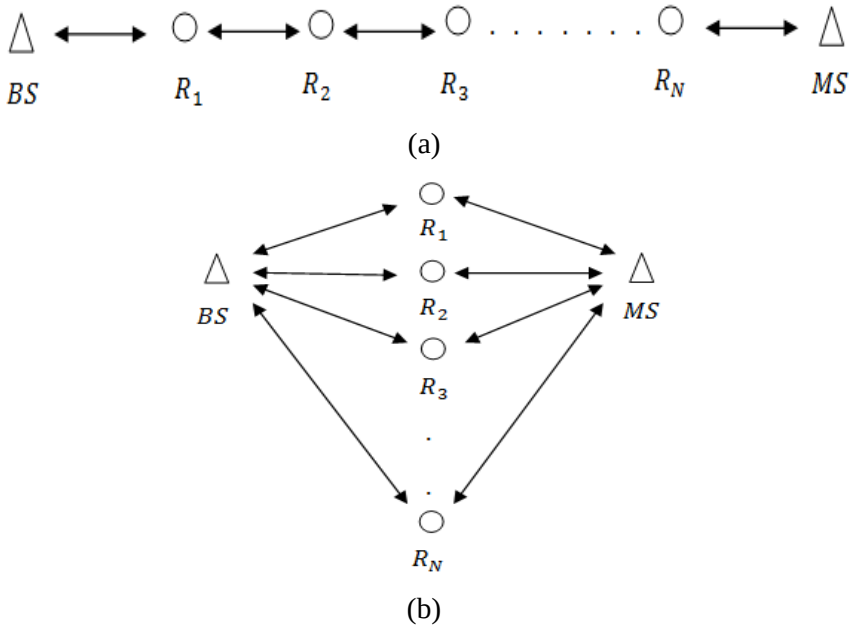

Fig. 1.5 Multiple relay nodes between BS and MS for (a) series configuration and (b) parallel configuration.

Initially, DASs were introduced for indoor communication in order to provide coverage to the dead spots within the building [34, 35]. The use of single antenna for indoor communication has been shown to be ineffective as the propagation loss and the delay spread were encountered in large buildings. Saleh et al [35] have proposed the solution to this problem by replacing the single antenna by DAS. The introduction of distributed ports has provided a significant advantage over coverage with simple processing devices such as amplifiers and down converters. However, the application of DASs has been further extended to different scenarios, exploiting their advantages of power saving and improved system capacity [36- 43]. Yanikomeroglu and Sousa [37] have introduced the architecture for the environment with high level of shadowing and have performed the analysis of indoor wireless CDMA communication system using distributed antennas. The applications have been investigated of CDMA personal communication services distributed antenna system in 1.8 GHz band [38]. The relationship between the numbers of antenna elements in CDMA distributed antenna system and reverse link SIR with the dynamic range of power control has been investigated [39]. Obaid and Yanikomeroglu

[40] have investigated the peak and median transmit power requirement in CDMA systems employing power control with distributed antenna architecture. In [41], the forward link and reverse link channel capacities have been analyzed with Maximal ratio combining (MRC) technique and the analytical expression for outage probability have also been derived. The reverse link capacity increases significantly as the macrodiversity technique employed suppresses the interference. However, there was no improvement over the forward link capacity. Furthermore, new transmission schemes were presented and have shown that forward link capacity increases with the number of distributed antennas in the system. The antenna architecture called CDMA sectorized distributed antenna (SDA) has been proposed to overcome the disadvantage of CDMA distributed antenna that is of low capacity per antenna element due to multiple access interference [42]. The power control algorithm that balances the SIR in CDMA sectorized distributed antenna system has been proposed [43].

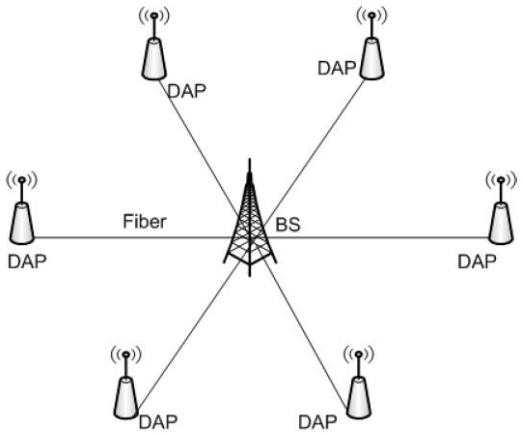

Fig.1.6 A typical distributed antenna system with six distributed antenna ports per cell [44].

Recently, the performance analysis or capacity analysis of DAS has been considered in equivalence to the two main models [44]. First considers DAS as the variation of conventional MIMO systems, where the antenna elements are distributed geographically [45]. However, there are certain differences between the DAS and the collocated MIMO systems such as the collocated MIMO systems have common power constraint and in DAS, each distributed port has their own power constraint. In addition to this, each distributed port in DAS has different channel gain as the user terminal and the distributed antenna ports experience different levels of multipath/small scale fading, shadowing and

path loss. Therefore, the analysis performed over DAS differs to that applied for conventional collocated MIMO systems.

Another model that can be considered equivalent to that of the DAS is of multi-cell processing. The multi-cell processing refers to the co-operative MIMO where the cooperating base stations are considered as DASs [46]. The cooperative approach is applicable when advance processing is considered at the distributed antenna port.

In DAS, communication is between geographically distributed antenna ports which experience different levels of small scale fading and large scale fading. Therefore, a composite fading model is required for the performance analysis of communication systems over distributed ports. However, the analysis is provided by considering the individual fading models and therefore will not result into accurate approximation of wireless channel over DAS. The performance analysis for ergodic and outage channel capacity over Generalized-k fading environment in DAS has been investigated [47]. Roh and Paulraj [48], has performed the channel capacity analysis for uplink and downlink with the assumption of constant path loss between the MS and the distributed port. Furthermore, composite channel model combining only fast fading and shadowing has been investigated [49]. However, the distances between the MS and the distributed port is usually different in practical scenario and therefore, the aforementioned assumption of taking path loss constant is not valid in case of DAS. The channel capacity performance for DAS has been further investigated without considering the effect of log-normal shadowing [50]. Zhu [51] has performed the analysis over spectral efficiency of DAS with the assumption that the shadowing effect was not considered. However, the distributed ports in DAS and therefore, must be considered in the composite fading model. The experimental measurements also verify that the small scale fading and shadowing occurs simultaneously in a practical wireless communication channel [11]. Nikolopolous et al [52] has investigated the narrowband fading by considering only the effect of fast fading. The channel models has been analyzed by combining the path loss, shadowing and Rayleigh fading environment [53- 55]. The system performance has been evaluated over composite shadowed Nakagami-m fading channel for DAS [56, 57]. It has been shown that the Rayleigh distribution and the Nakagami-m distribution can be

generalized as special cases of the Generalized Gamma distribution [58]. Therefore, we can generalize the small scale fading effect with Generalized Gamma distribution.

1.1.3 Composite fading models

The communication between distributed ports has lead to the consideration of composite fading models for analysis of wireless communication channel. The aforementioned statistical models independently model various types of fading considering only one type of fading irrespective of the others for modeling and therefore will not give accurate approximation for wireless channel and thus performance analysis of wireless communication systems would not be reliable. Also, as we are moving to communication over distributed ports or nodes, the use of composite fading model comes into role as distributed nodes or ports experience different level of fading and shadowing. To have a better approximation of wireless channel we need to consider all categories of fading simultaneously which forms the basis for requirement of a composite model. In most of the cases for composite fading models, received power variation due to path loss is assumed to be identical and can be ignored while forming a composite model as distance between the transmitter and the receiver is assumed to be known always. The combined effect of shadowing and multipath is obtained from their joint distribution. However, these composite models have a complicated integral form.

Simon and Alouini [59], have unified the bit error rate performance of digital communication systems for coherent, differentially coherent and non coherent forms of detection over different fading channels by utilizing the alternate representation of Gaussian and Marcum Q-functions. The derived error rate expressions were in the form of a single integral with finite limits and integrand composed of elementary functions that can be numerically evaluated.

The composite fading model is obtained by the joint distribution of multipath fading distribution and that of the shadowing distribution. Therefore, we have Rayleigh-lognormal, Nakagami-lognormal or weibull- distributions as a composite fading model.

Shen et al [60] has performed channel capacity analysis for multiple input multiple output (MIMO) channels over Rayleigh-lognormal fading environment and derived the

analytical expressions using Gaussian-Laguerre numerical integration and Gaussian-Hermite numerical integration.

The second order statistics of the received signal envelope have been provided in Weibull-Lognormal fading environment [61, 62]. Karadimas and Kotsopoulos [61], have investigated the effect of inhomogeneous scattering in the channel and the shadowing effect by using Weibull-Lognormal distribution where, Weibull distribution is used to model the non-uniformities of the scatterers and lognormal distribution is used to model shadowing that is the slow variation of the mean. The approximate solution to second order statistics have been provided for level crossing rate (LCR) and average duration of fade (ADF) using the Weibull-Lognormal distribution. Gaber et al [63], have provided outage probability analysis for cooperative diversity wireless networks using amplify and forward relays over independent and not identically distributed weibull and Weibull-Lognormal for single and multiple relays. The PDF of received SNR have been approximated by some lower bounds and closed form expression for MGF of received SNR in terms of MeijerG has also been derived. The analytical results have been provided and validated the potential gain of relaying techniques over the outage probability.

Tjhung and Chai [64], have derived the expressions for average level crossing rate (LCR) and average time fade duration (AFD) in microcellular mobile radio channels using Nakagami distribution for fading and lognormal distribution for shadowing. The performance analysis for adaptive transmission system over MRC combining technique using Nakagami-Lognormal distribution has been provided. Closed form expressions for throughput and outage probability have been derived and the effect of different parameters of Nakagami-Lognormal distribution on adaptive transmission system has been analyzed [65].

The aforementioned literature shows the composite fading models with combined effect of multipath/small scale fading and shadowing where, shadowing is modeled by lognormal distribution. However, their complex integral form has made these distributions cumbersome for analysis of wireless channel. This has motivated for the introduction of some simpler approximate distributions to model composite fading

channel where, multipath is superimposed on shadowing. Abdi and Kaveh [66], has accurately approximated Rayleigh-Lognormal distribution by K distribution, which is a mixture of Rayleigh and Gamma distributions. This approximation resulted from the fact that Gamma distribution closely approximates to Log normal distribution and hence can replace Log normal distribution from the composite model and thus simplifying the integral. Abdi and Kaveh [67], has derived the bit error rate (BER) for Differential phase shift keying (DPSK) and minimum shift keying (MSK) for K distribution and has shown the numerical equivalence of results obtained for K distribution and those for Rayleigh-Lognormal distribution. The K-distribution is used in place of Rayleigh-Lognormal distribution for analytical calculations as gamma distribution instead of lognormal distribution is used to model shadow fading. Iskander et al [68], has estimated the parameters of K-distribution by using combination of maximum likelihood and the method of moments which has resulted in lowest variance of parameter estimates as compared to existing non maximum likelihood techniques. The derived approach leads to low computational difficulty and estimation has lower mean square error as compared to methods based on second and fourth order moments. Mathematical maximum likelihood relationship between shape parameter and scale parameter has been derived using log-likelihood function derivative of generalized Bessel function K (GBK) distribution and are useful in radar applications. Theofilakos et al [69], has obtained analytical expressions for moment generating function (MGF) and marginal moment generating function (MMGF) for k-distribution with fading parameter k having the values of a positive integer plus half and has performed the analysis of generalized selection combining (GSC) receivers over independent and identically distributed (iid) k fading channels. Average symbol error probability (ASEP) has been evaluated for coherent M-ary phase shift keying (MPSK) with GSC receivers using obtained MMGF expression.

1.1.4 Generalized-K Fading

The aforementioned expression for K distribution is generalized by replacing Rayleigh distribution by Nakagami-m distribution, which can model different levels of fading. This generalized case is defined as Generalized K fading. Shankar [70] has developed a mathematical expression for the probability distribution function (PDF) of Generalized-K

fading and its amount of fading (AF). Variation of average probability of error for binary phase shift keying (BPSK) in presence of fading and shadowing was plotted with respect to average signal to noise ratio (SNR). However, SNR statistics for generalized k fading were still not available and which was given by Bithas et al [71].

The PDF for received SNR over Generalized-K fading is given as [71]

$$f_\gamma(\gamma) = \frac{2\Xi^{\frac{(\beta+1)}{2}}\gamma^{\frac{(\beta-1)}{2}}}{\Gamma(m)\Gamma(k)} K_\alpha\left(2\sqrt{\Xi\gamma}\right) \qquad \gamma \geq 0 \tag{1.10}$$

where, $\Xi = \frac{km}{\bar{\gamma}}$, $\alpha = k - m$ and $\beta = k + m - 1$. $\bar{\gamma}$ is the average received SNR, k and m are the shadowing and fading parameters, respectively. $K_\alpha(.)$ is the modified Bessel function of second kind of order α and $\Gamma(.)$ is the gamma function.

The amount of fading (AoF) for generalized-k fading is given as [70]

$$AoF = \frac{1}{m} + \frac{1}{k} + \frac{1}{mk} \tag{1.11}$$

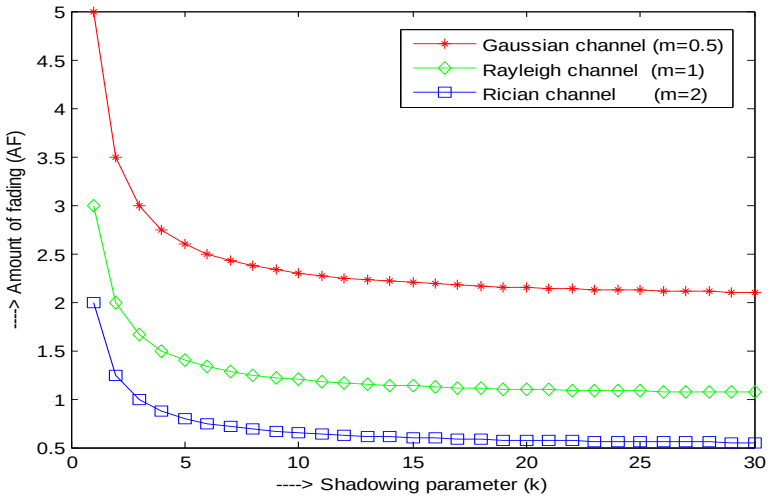

Fig. 1.7 The amount of fading variations over Generalized-K fading with respect to shadowing parameter and for different values of fading parameter.

Figure shows the variation of fading level with respect to shadowing and fading parameter. Therefore, it is validated that the level of fading decreases with the higher values of fading and shadowing parameter. Rician channel with LOS has lowest amount of fading as compared to Rayleigh and Gaussian fading channel. The performance

analysis over a fading channel mainly comprises of bit error rate (BER) analysis, outage probability and channel capacity. Several papers concerning the analysis for single input single output (SISO) and single input multiple output (SIMO) over fading channels has been introduced [72- 77]. The closed form expressions for channel capacity over Nakagami-m fading channel has been proposed based on Moschopoulos series [72]. In [73], the ergodic Shannon capacity for fading channels has been proposed over Rayeigh distribution with and without diversity combining technique. The results of [73] have been extended to Rician and Nakagami-m distributions [74]. There are various approaches that can be exploited for performance analysis such as PDF based, CF based and MGF based approach. The CF-based approach has been used to compute the ergodic channel capacity over Nakagami-m fading channel for SIMO systems [75]. The Shannon capacity for SISO systems by using the properties of MeijerG function over Generalized-K fading environment has been computed in [76].The MGF based approach has been exploited for the ergodic capacity analysis of MRC diversity combining technique for correlated Rician fading channel [77].

The MGF based approach provides significant advantage over the PDF based approach in reference to the performance analysis. For instance, the BER analysis for binary phase shift keying (BPSK) using PDF based approach comprises of integral involving error function [70] and on the contrary, the MGF based approach result into closed form expression for the BER [78]. Therefore, simplification over the performance analysis can be achieved using MGF based approach by exploiting the alternate form of Q-function and the properties of Laplace transform. The figure shows the BER analysis for PDF based and MGF based approach for BPSK modulation techniques. The expressions for both the approaches are provided in appendix A.

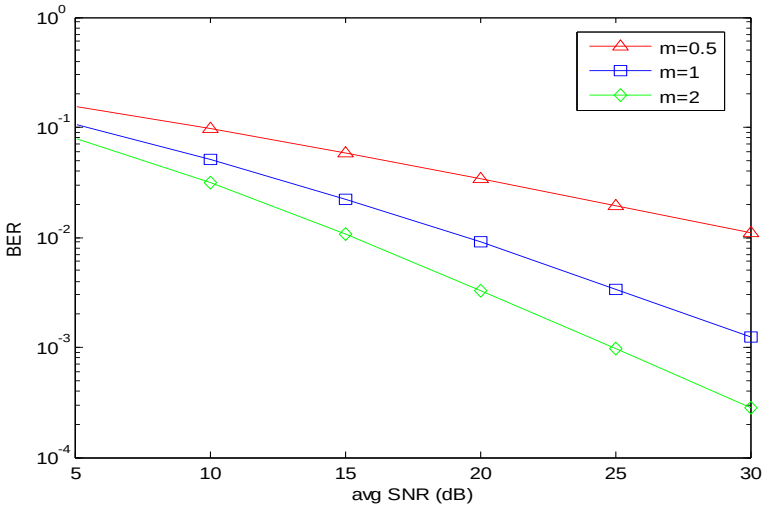

Fig. 1.8 BER vs average SNR over Generalized-K fading channel for different fading levels and fixed value of shadowing parameter (k=1.0931) using PDF based approach [70].

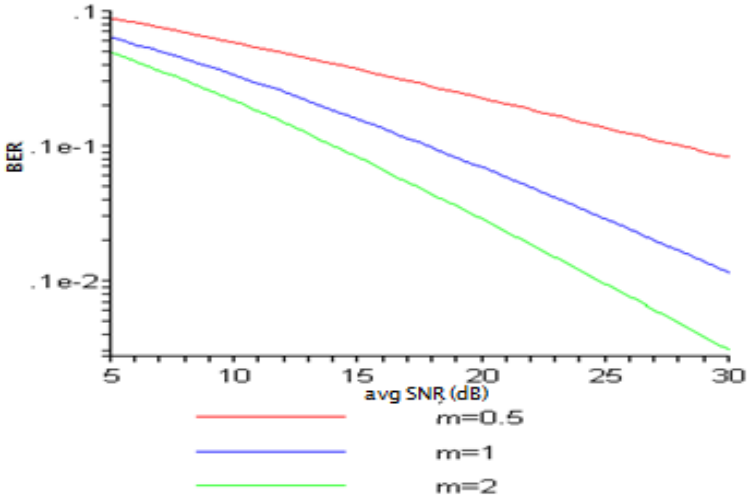

Fig. 1.9 BER vs average SNR over Generalized-K fading channel for different fading levels and fixed value of shadowing parameter (k=1.0931) using MGF based approach [78].

Expressions for cumulative distribution function (CDF) in terms of generalized Hypergeometric function and moment generating function (MGF) in terms of Whittaker function [14, eq. (9.220)] were provided. Analysis of digital communications over Generalized K fading was done by calculating nth order moment, average symbol error probability (SEP) for different modulation techniques by averaging the conditional symbol error probability over the PDF of SNR, outage probability and channel capacity . Outage probability was plotted with respect to normalized threshold SNR for several

values of k and m and it was shown that as the values of k and/or m increases, outage probability decreases. Normalized channel capacity was plotted as a function of average received SNR for different values of k and m and it was shown that capacity improves as k and/or m increase. In [79], Kostic has presented a new Fourier series form probability density function (PDF) for the phase of the received signal over Generalized K fading channel with additive Gaussian noise. An alternate new closed form expression for binary composite phase shift keying (CPSK) was evaluated and the results were compared with that of the Fourier series form phase PDF and were found to be equivalent. Efthymoglou [80] has derived symbol error rate (SER) for different modulation schemes using MGF based approach for arbitrary values of fading parameter m and shadowing parameter k in case of Generalized K fading. Also, CDF was obtained in terms of Bessel K function [14, eq. (8.407.1)] for integer values of m in Generalized K fading. Expressions for outage probability, BER for various binary and multilevel modulation techniques and average channel capacity were derived, with m having integer values. Bithas et al [71], has derived the closed form expressions for the outage probability, BER analysis and average channel capacity. Outage probability is defined as the probability that the received SNR falls below a certain threshold value (γ_o) and is given as [11]

$$P_{out} = P(\gamma \leq \gamma_o) \tag{1.12}$$

$$P_{out} = \int_0^{\gamma_o} P_\gamma(\gamma) d\gamma \tag{1.13}$$

For generalized k-fading outage probability is given as

$$P_{out} = \int_0^{\gamma_o} \frac{2\Xi^{\frac{(\beta+1)}{2}} \gamma^{\frac{(\beta-1)}{2}}}{\Gamma(m)\,\Gamma(k)} K_\alpha(2\sqrt{\Xi\gamma}) d\gamma \tag{1.14}$$

The performance of fading channel improves with the increase in fading and shadowing parameter. The outage probability variation with respect to normalized threshold SNR is shown in Fig. 1.10 for different levels of fading and shadowing. The threshold SNR defines the cut off value for SNR below which communication between the transmitter and the receiver is not established. Therefore, the probability of the system to be in outage is unity for the values of threshold SNR greater than the average SNR [87].

However, as the average SNR exceeds the value of threshold SNR, the outage probability decreases as is validated from the figure.

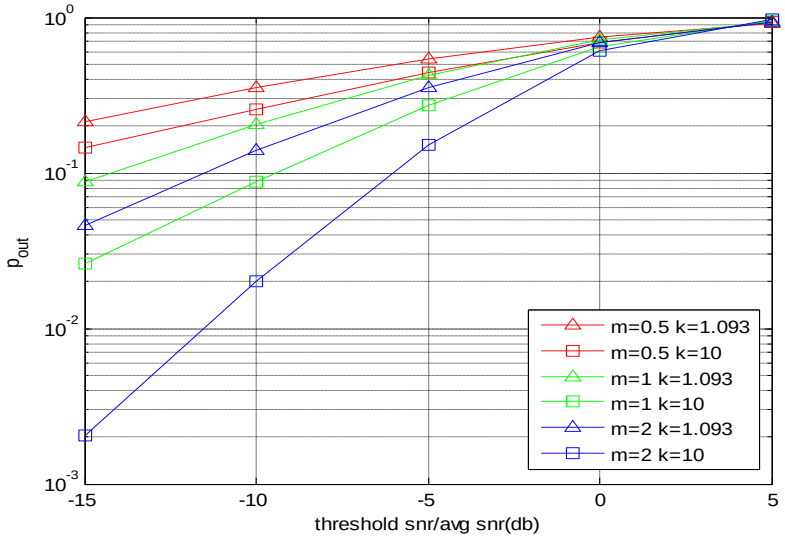

Fig.1.10 The response for outage probability with respect to normalized threshold SNR over Generalized-K fading environment for different values of fading (m=0.5, 1 and 2) and shadowing parameter (k=1.0931 and 75.11) [71].

Degrading effects of multipath fading in digital wireless communications are prevented by utilizing Diversity combining techniques [2]. Different types of receiver diversity combining techniques are Selection combining (SC), Maximal ratio combining (MRC) and Equal gain combining (EGC). Performance of diversity combining over composite fading is available in literature. In [25], Ricean and Suzuki distributions were used to model the land-mobile satellite channel and performance evaluation of M-ary phase shift keying (PSK) and M-ary differential phase shift keying (DPSK) using micro-diversity reception technique was studied for SC and MRC. The improvement over channel capacity is provided by exploiting the channel state information (CSI) at transmitter. The transmitter by making use of available CSI adapts its transmission rate, power or coding techniques in order to have improvement over the capacity gain. Laourine et al. [81], has obtained closed form expressions for capacity of generalized k-fading under three different adaptive transmission techniques namely optimal rate adaptation with constant transmit power (C_{ORA}), optimal simultaneous rate and power adaptation (C_{OPRA}) and channel inversion with fixed rate (C_{CIFR}) and has compared the results with numerical

simulations. Efthymoglou et al. [82] has derived analytical closed form expressions for outage probability, average BER for different modulation schemes and channel capacity under different adaptive techniques, namely channel capacity with optimal rate adaptation and fixed transmit power (C_{ORA}), channel capacity with optimal simultaneous rate and power adaptation (C_{OPRA}), channel capacity with channel inversion and fixed rate (C_{CIFR}) and channel capacity with truncated channel inversion and fixed rate (C_{TCIFR}) in terms of generalized Hypergeometric function. However, functions are not defined for integer values of (k-m). Renzo et al. [83], has obtained a novel and unified analysis of channel capacity using some special transforms. The E_i transform has been used to compute channel capacity with side information at receiver by MGF of SNR and channel capacity with side information at transmitter and receiver by truncated MGF of SNR at receiver, whereas, Mellin and Hankel transform of MGF of received SNR has been used to obtain channel capacity with channel inversion and truncated channel inversion respectively. Higher order statistics (HOS) has been introduced for channel capacity with side information at receiver and has compared the simulation results with that of the analytical one. Dwivedi and Singh [78], has obtained the closed form expression for average BER of BPSK/ BFSK and average SER for rectangular quadrature amplitude modulation scheme using Moment Generating Function (MGF) in terms of Meijer G over generalized-K fading channels. Mathematical expressions for outage probability and channel capacity for channel inversion with fixed rate has also been derived and plotted. Average BER and outage probability results with proposed approach has been compared to the PDF based approach and found to be equivalent. Cao [84], has provided SER and outage performance analysis for multiple links over generalized-K fading channel using PDF of end to end SNR and also provided analytical expressions for second order statistics such as level crossing rate (LCR) and average outage duration (AOD). Analytical results have been justified by simulation results and optimum number of hops for a given distance of transmission link and channel fading parameters has also been provided. Yilmaz and Alouini [85], has computed average channel capacity under an unified framework for two diversity combining techniques namely Equal Gain Combining (EGC) and maximal ratio combining (MRC) and has derived a novel closed form expression for MGF for Generalized k fading.

1.2 Problem statement

The wireless communication channel is highly indeterministic in nature and therefore, poses difficulty in its simulation. The radio waves propagating through the wireless channel undergo various mechanisms such as reflection, diffraction and scattering which result into low signal power at receiver. This random variation in received signal power is termed as fading and is an important parameter for wireless channel. Furthermore, fading in wireless communication channel is categorized on the basis of distance at which the signal variation occurs as Large scale fading and Small scale fading. The performance analysis of digital communication systems over fading channels usually, model the wireless channel with individual effects of fading. However, in practical scenarios the small scale fading is superimposed by the effect of shadowing and path loss. Therefore, the channel modeling with individual fading environment is not an accurate approximation to the wireless channel. This has resulted into consideration of composite fading model. In addition to the aforementioned discussion, the next generation communication system is moving towards the distributed communication with collocated distributed antenna system (DAS) or co-operative network within neighbouring cell and therefore, has motivated for the requirement of composite fading model comprising of both large scale and small scale fading. This motivation has resulted from the fact that the distributed ports in a DAS are extended geographically over the large area and therefore the shadowing variation would be different for each distributed port and cannot be ignored. However, the distance between the receiver and the distributed ports is different and therefore, path loss for each communication link would be different. Thus, the channel model for the DAS requires a composite fading model combining the effect of path loss, shadowing and fading. This has been considered as the problem statement for the work and therefore composite model with combination of small scale fading and shadowing is provided with Generalized-K fading and performance analysis is performed.

In view to performance analysis, the MGF based approach is used for the analysis as MGF based approach results into simple closed form expression and therefore, unification of performance analysis is required under MGF based approach. The channel

capacity is considered as the important performance metric for wireless channel and therefore, improvement over the channel capacity is provided by exploiting CSI at the transmitter. The channel capacity with optimal rate adaptation, optimal simultaneous power and rate adaptation and channel inversion with fixed rate has been discussed in literature with both PDF and MGF based approach. However, the performance analysis of the channel capacity under truncated channel inversion with fixed rate over Generalized-K fading channel is presented as the work of this dissertation.

Furthermore, the DAS has evolved as the new technology in wireless communication systems in order to have improved cell edge coverage, outage performance and channel capacity. Therefore, the analysis of DAS has been considered. The closed form approximate model for outage and channel capacity analysis for DAS with fixed and transparent relaying techniques over composite fading channel combining path loss, shadowing and fading is provided for single node relaying and multiple nodes relaying.

1.3 Dissertation outline

The dissertation outline is as follows. This chapter provides the introduction to fading phenomenon and the various channel models available for fading environment. The basic idea for DAS has been provided with different relaying configuration and the need for composite fading model is being discussed. In addition to the system model, introduction to composite fading model using Generalized-K fading and the literature review for its analysis has been provided.

Chapter 2 describes the channel capacity analysis over Generalized-K fading environment with adaptive techniques exploiting the CSI at the transmitter. The channel model for the wireless communication system using Generalized-K distribution has been provided. Furthermore, closed form expressions and the mathematical analysis of the channel capacity for suboptimal adaptive technique such as channel inversion with fixed rate (C_{CIFR}) and truncated channel inversion with fixed rate (C_{TCIFR}) using MMGF based approach has been provided.

Chapter 3 describes the channel capacity and outage probability analysis for DAS with fixed and transparent relays over the composite fading channel model using the joint distribution of generalized Gamma, lognormal and path loss distribution. In this chapter, we have derived analytical expressions for the outage probability and the downlink channel capacity for composite fading environment between DA and MS. However, the numerically simulated results have been provided for transmission with single relay node as well as with multiple relay nodes between the transmitter and the receiver. The system model consists of N number of distributed antennas per cell connected to the BS serving a single user at arbitrary location. The analytical expression for channel capacity and the outage probability were approximated by using Gauss-Hermite quadrature integral for the proposed DAS.

Chapter 4 represents the diversity combining techniques at the receiver and its advantages over mitigating the effect of channel fading over Generalized-K fading. The maximal ratio combining receiver is considered to have the better performance over selection combining and the equal gain combining. Therefore, analytical expression for channel capacity under truncated channel inversion with fixed rate using MRC diversity combining technique at receiver has been provided and the performance analysis over multiple links has been provided.

Finally, chapter 5 concludes the work and provides the future scope for the dissertation.

CHAPTER 2

CHANNEL CAPACITY WITH SUBOPTIMAL ADAPTATION TECHNIQUE OVER GENERALIZED-K FADING

2.1 Introduction

The channel capacity is the most important performance metric for wireless communication channel. Shannon [85] has evaluated the channel capacity for additive white Gaussian noise (AWGN) channel. However, it cannot be used directly for fading channel, leading to the case of average capacity that is the average of Shannon's capacity over the distribution of received SNR. However, the significant improvement in channel capacity for fading channel is obtained by the use of channel state information (CSI) at transmitter which can now adapt its transmission strategy, that is, transmission rate, power and coding techniques in accordance to the channel variations [87, 88]. Therefore, based on different adaptive techniques, several categories of the channel capacity have been classified such as: 1) channel capacity with optimal rate adaptation and fixed power (C_{ORA}), 2) channel capacity with simultaneous power and rate adaptation (C_{OPRA}), 3) channel capacity with channel inversion and fixed rate (C_{CIFR}), and 4) channel capacity with truncated channel inversion and fixed rate (C_{TCIFR}) [87]. The first two adaptation techniques refers to optimal adaptation techniques as both power and transmission rate is adapted in accordance to CSI and the latter two are defined as sub optimal adaptation technique as only transmitting power is being adapted with reference to the CSI. Laourine et al [81] have evaluated the channel capacity with the aforementioned adaptive techniques using PDF based approach over Generalized-K fading environment. Efthymoglou et al [82] have derived closed form expressions for bit error probabilities over different modulation techniques as well as channel capacity of aforementioned adaptation techniques for Generalized-K fading environment. However, PDF based capacity analysis has complex forms and therefore MGF based approach has been

introduced. Renzo et al [83], have provided MGF based approach for performance analysis of wireless communication channels. However, the analysis provided is quite lengthy. Recently, the marginal moment generating function (MMGF) based performance analysis over correlated Nakagami-m fading with maximal ratio combining (MRC) have been provided [89]. Dwivedi et al [78], have reported closed form expression for channel capacity with channel inversion and fixed rate over Generalized-K fading using MGF. However, with best of author's knowledge, the channel capacity for truncated channel inversion with fixed rate over Generalized-K fading has not been reported. This has provided a general framework to compute the MMGF for Generalized-K distribution and is further used to compute the channel capacity for channel inversion and truncated channel inversion.

2.2 Generalized-K Fading Channel Model

The Generalized-K distribution is the joint distribution of Nakagami-*m* and Gamma distribution which are used to model the multipath fading and shadowing, respectively. However, it is the most generalized case as it can model various fading levels by a sheer change in its shaping parameters. The PDF of received SNR over the Generalized-K distribution is given as [71]:

$$f_\gamma(\gamma) = \frac{2\Xi^{\frac{(\beta+1)}{2}}\gamma^{\frac{(\beta-1)}{2}}}{\Gamma(m)\Gamma(k)} K_\alpha\left(2\sqrt{\Xi\gamma}\right) \qquad \gamma \geq 0 \tag{2.1}$$

where, $\Xi = \frac{km}{\bar{\gamma}}$, $\alpha = k - m$ and $\beta = k + m - 1$. $\bar{\gamma}$ is the average received SNR, k and m are the shadowing and fading parameters, respectively. $K_\alpha(.)$ is the modified Bessel function of second kind of order α and $\Gamma(.)$ is the gamma function. The amount of fading (AoF) for generalized-k fading is given as $AoF = \frac{1}{m} + \frac{1}{k} + \frac{1}{mk}$ [70].Which reveals that, it has an inverse relation to the fading and shadowing parameter. In general, m = 0.5, 1 and 2 represent one sided Gaussian, Rayleigh and Rician distributions and k =1.0931, 75.11 represent the heavy and light shadowing, respectively [11, 81].

2.3 Marginal Moment Generating Function

However, most framework described for the analysis of spectral efficiency over fading channels in various literature make use of the so-called PDF based approach of the received SNR, which is a task that might be very cumbersome for system setups and often require to manage mathematical expressions. It is also well known fact that the prior knowledge of the CSI at the transmitter is exploited to improve the channel capacity. The MGF and the characteristic function (CHF) based approaches have extensively been used for analyzing the average bit-error-rate probability and outage probability. Alouini et al [72] have also pointed out the complexity of using MGF and CHF based approaches for the computation of the channel capacity. Moreover, the application of PDF based approach for computation of the channel capacity appear to be in evident counter tendency with recent advances on performance analysis of the digital communication over fading channels. Several researchers [90- 92] have demonstrated the significance of using either MGF or CHF based approach for simplifying the analysis in most situation of interest for the computation of important performance metrics, whereas the application of PDF based approach seems impractical. Recent advances in the performance analysis of digital communication systems in the fading environment has recognized the potential importance of the MGF or Laplace transforms as a powerful tools for simplifying the analysis of diversity communication systems. This led to a simple expression to average bit-error-rate and symbol-error-rate for wide variety of digital communication scheme on fading channels including multipath reception with correlated diversity [93, 94]. Theofilakos et al [69] have evaluated the MMGF and further used it for the evaluation of bit-error-rate. In this section, MMGF is evaluated for Generalized-K fading and further, it is used for computation of the channel capacity. The moment generating function is closely related to the Laplace transform and is given as expectation of $e^{s\gamma}$ and when this expectation is taken above a certain cut off value; we have marginal moment generating function, defined as [69]:

$$\widehat{M}(-s,a) = \int_a^{\infty} e^{-s\gamma} f_{\gamma}(\gamma)\, d\gamma \tag{2.2}$$

After substituting the value of $f_{\gamma}(\gamma)$ from Eq.(2.1), we get:

$$\widehat{M}(-s,\gamma_o) = \int_{\gamma_o}^{\infty} e^{-s\gamma} \frac{2\Xi^{\frac{(\beta+1)}{2}} \gamma^{\frac{(\beta-1)}{2}}}{\Gamma(m)\Gamma(k)} K_{\alpha}\left(2\sqrt{\Xi\gamma}\right) d\gamma \tag{2.3}$$

By substituting, $2\sqrt{\Xi\gamma}$ = t in Eq.(2.3), we get:

$$\widehat{M}(-s,\gamma_o) = \frac{1}{2^{\beta-1}\Gamma(m)\Gamma(k)} \int_{2\sqrt{\Xi\gamma_o}}^{\infty} t^{\beta} e^{\frac{-st^2}{4\Xi}} K_{\alpha}(t)\, dt \tag{2.4}$$

Now, $K_{\alpha}(t)$ in terms of generalized hypergeometric function is written as [23]:

$$K_{\alpha}(t) = \pi \csc(\alpha\pi)\left(2^{\alpha-1}t^{-\alpha}\ {}_0F_1\left(;1-\alpha;\frac{t^2}{4}\right) - 2^{-\alpha-1}t^{\alpha}\ {}_0F_1\left(;\alpha+1;\frac{t^2}{4}\right)\right) \tag{2.5}$$

where, ${}_0F_1$ is the Generalized Hypergeometric function and is written in the series form as [95]:

$${}_0F_1(;b;z) = \sum_{p=0}^{\infty} \frac{z^p}{(b)_p\, p!} \tag{2.6}$$

Using Eq.(2.5) and Eq.(2.6), Eq.(2.4) can be written as:

$$\widehat{M}(-s,\gamma_o) = \frac{\pi \csc(\alpha\pi)}{2^{\beta-1}\Gamma(m)\Gamma(k)} \int_{2\sqrt{\Xi\gamma_o}}^{\infty} t^{\beta} e^{\frac{-st^2}{4\Xi}} \left(2^{\alpha-1}t^{-\alpha}\ \sum_{p=0}^{\infty} \frac{t^{2p}}{4^p\Gamma(p-\alpha+1)p!} - 2^{-\alpha-1}t^{\alpha} \sum_{p=0}^{\infty} \frac{t^{2p}}{4^p\Gamma(p+\alpha+1)p!}\right) dt$$

$$\widehat{M}(-s,\gamma_o) = \frac{\pi \csc(\alpha\pi)}{\Gamma(m)\Gamma(k)} \left[2^{\alpha-\beta} \sum_{p=0}^{\infty} \frac{1}{4^p\Gamma(p-\alpha+1)p!} I_1 - 2^{-\alpha-\beta} \sum_{p=0}^{\infty} \frac{1}{4^p\Gamma(p+\alpha+1)p!} I_2\right] \tag{2.7}$$

where,

$$I_1 = \int_{2\sqrt{\Xi\gamma_o}}^{\infty} t^{\beta-\alpha+2p} e^{\frac{-st^2}{4\Xi}} dt \tag{2.8}$$

and

$$I_2 = \int_{2\sqrt{\Xi\gamma_o}}^{\infty} t^{\beta+\alpha+2p} e^{\frac{-st^2}{4\Xi}} dt \tag{2.9}$$

Again by change of the variables, $t = 2\sqrt{\Xi\gamma}$ in Eq.(2.8) and Eq.(2.9) and using [14, Eq.(3.381.3)], we have:

$$I_1 = 2^{\beta-\alpha+2p}\ \Xi^{\frac{\beta-\alpha+2p+1}{2}} s^{\frac{-\beta+\alpha-2p-1}{2}} \Gamma\left(\frac{\beta-\alpha+2p+1}{2}, s\gamma_o\right) \tag{2.10}$$

and

$$I_2 = 2^{\beta+\alpha+2p}\ \Xi^{\frac{\beta+\alpha+2p+1}{2}} s^{\frac{-\beta-\alpha-2p-1}{2}} \Gamma\left(\frac{\beta+\alpha+2p+1}{2}, s\gamma_o\right) \tag{2.11}$$

By substituting the values from Eq.(10) and Eq.(11) in Eq.(7) and after some mathematical manipulations, we have MMGF as:

$$\widehat{M}(-s,\gamma_o) = \frac{\pi \csc(\alpha\pi)}{\Gamma(m)\Gamma(k)}\left\{\sum_{p=0}^{\infty} \frac{1}{\Gamma(p-\alpha+1)p!}\left(\Xi/s\right)^{\frac{\beta-\alpha+2p+1}{2}} \Gamma\left(\frac{\beta-\alpha+2p+1}{2}, s\gamma_o\right) - \right.$$

$$\left. \sum_{p=0}^{\infty} \frac{1}{\Gamma(p+\alpha+1)p!}\left(\Xi/s\right)^{\frac{\beta+\alpha+2p+1}{2}} \Gamma\left(\frac{\beta+\alpha+2p+1}{2}, s\gamma_o\right)\right\} \tag{2.12}$$

This provides the required mathematical expression for MMGF of Generalized-K fading.

2.4 Channel Capacity Analysis

The channel capacity has been regarded as the fundamental information theoretic performance measure to predict the maximum information rate of a communication system. It is extensively used as the basic tool for the analysis and design of more efficient techniques to improve the spectral efficiency of the modern wireless communication systems and to gain insight into how to counteract the detrimental effects of the multipath fading propagation via opportunistic and adaptive communication methods. Shannon [85] has evaluated the channel capacity for additive white Gaussian noise (AWGN) channel. However, it cannot be used directly for fading channel, leading to the case of ergodic capacity, which is the average of Shannon's capacity over the distribution of received SNR. This average capacity is improved by using CSI at transmitter, which is made available at transmitter by the receiver through a feedback path. In this analysis, we have considered that the transmitter is having perfect CSI and based on this the transmitter now adapts its transmission rate, power and coding techniques to have various optimal and suboptimal adaptation techniques, namely, C_{ORA}, C_{OPRA}, C_{CIFR} and C_{TCIFR}. In C_{ORA} only the transmission rate is varied in accordance to CSI keeping power constant and for C_{OPRA} both power and rate are varied, simultaneously. In C_{CIFR}, the transmitter adapts its transmission power in such a way that

constant SNR is maintained at the receiver with a fixed transmission rate, that is the channel fading effects are assumed to be inverted. Therefore, the receiver assumes fading channel to be time invariant AWGN channel and if the channel fading effect is inverted above a certain threshold value, then we have channel capacity under truncated channel inversion with fixed rate. The channel capacity for suboptimal adaptation technique in terms of PDF of received SNR is given as [94].

$$C_{CIFR} = Blog_2\left(1 + \frac{1}{\int_0^{\infty} \frac{f_\gamma(\gamma)}{\gamma} d\gamma}\right) \tag{2.13}$$

and

$$C_{TCIFR} = Blog_2\left(1 + \frac{1}{\int_{\gamma_o}^{\infty} \frac{f_\gamma(\gamma)}{\gamma} d\gamma}\right)(1 - P_{out}) \tag{2.14}$$

where, P_{out} = the outage probability and B is the channel bandwidth. By replacing, $\frac{1}{\gamma} = \int_0^{\infty} e^{-s\gamma}\, ds$ and changing the order of integral, we have channel capacity in terms of MMGF as:

$$C_{CIFR} = Blog_2\left(1 + \frac{1}{\int_0^{\infty} \bar{M}(-s,0) d\gamma}\right) \tag{2.15}$$

and

$$C_{TCIFR} = Blog_2\left(1 + \frac{1}{\int_0^{\infty} \bar{M}(-s,\gamma_o) d\gamma}\right)(1 - P_{out}) \tag{2.16}$$

By substituting the value of MMGF from Eq.(2.12) and evaluating the integral as:

$$I = \frac{\pi \csc(\alpha\pi)}{2^{\beta-1}\Gamma(m)\Gamma(k)}\left[\sum_{p=0}^{\infty} \frac{1}{\Gamma(p-\alpha+1)p!} \Xi^{\frac{\beta-\alpha+2p+1}{2}} I_3 - \sum_{p=0}^{\infty} \frac{1}{\Gamma(p+\alpha+1)p!} \Xi^{\frac{\beta+\alpha+2p+1}{2}} I_4\right] \tag{2.17}$$

where,

$$I_3 = \int_0^{\infty} s^{-\left(\frac{\beta-\alpha+2p+1}{2}\right)} \Gamma\left(\frac{\beta-\alpha+2p+1}{2}, s\gamma_o\right) ds \tag{2.18}$$

and

$$I_4 = \int_0^{\infty} s^{-\left(\frac{\beta+\alpha+2p+1}{2}\right)} \Gamma\left(\frac{\beta+\alpha+2p+1}{2}, s\gamma_o\right) ds \tag{2.19}$$

Using [96, Eq. (8.4.16.2)] and [96, Eq. (2.24.2.1)], we have:

$$I_3 = \gamma_o^{\left(\frac{\beta-\alpha+2p-1}{2}\right)} \frac{\Gamma\left(\frac{1-(\beta-\alpha+2p)}{2}\right)}{\Gamma\left(1+\frac{1-(\beta-\alpha+2p)}{2}\right)} \tag{2.20}$$

and

$$I_4 = \gamma_o^{\left(\frac{\beta+\alpha+2p-1}{2}\right)} \frac{\Gamma\left(\frac{1-(\beta+\alpha+2p)}{2}\right)}{\Gamma\left(1+\frac{1-(\beta+\alpha+2p)}{2}\right)} \tag{2.21}$$

By putting Eq.(2.20) and Eq.(2.21) in Eq.(2.17), we get:

$$I = \frac{\pi \csc(\alpha\pi)}{\Gamma(m)\Gamma(k)} \left[\sum_{p=0}^{\infty} \frac{\gamma_o^{\left(\frac{\beta-\alpha+2p-1}{2}\right)}}{\Gamma(p-\alpha+1)p!} \Xi^{\frac{\beta-\alpha+2p+1}{2}} \frac{\Gamma\left(\frac{1-(\beta-\alpha+2p)}{2}\right)}{\Gamma\left(1+\frac{1-(\beta-\alpha+2p)}{2}\right)} - \sum_{p=0}^{\infty} \frac{\gamma_o^{\left(\frac{\beta+\alpha+2p-1}{2}\right)}}{\Gamma(p+\alpha+1)p!} \Xi^{\frac{\beta+\alpha+2p+1}{2}} \frac{\Gamma\left(\frac{1-(\beta+\alpha+2p)}{2}\right)}{\Gamma\left(1+\frac{1-(\beta+\alpha+2p)}{2}\right)} \right] \tag{2.22}$$

The outage probability is defined as the probability that the received SNR falls below a certain threshold value and is given as [71, 78]:

$$P_{out} = P(\gamma \leq \gamma_o) \tag{2.23}$$

$$P_{out} = 1 - \frac{(\Xi\gamma_o)^{\frac{(\beta+1)}{2}}}{\Gamma(m)\Gamma(k)} G_{1,3}^{3,0}\left[\Xi\gamma_o, \begin{matrix} (1-\beta)/2 \\ -(1+\beta)/2 \quad \alpha/2 \quad -\alpha/2 \end{matrix} \right] \tag{2.24}$$

By using Eq.(2.22) and Eq.(2.24) in Eq.(2.15) and Eq.(2.16), we have achieved the channel capacity under channel inversion with fixed rate and truncated channel inversion with fixed rate over the Generalized-K environment, respectively, where the special functions can be easily evaluated by using mathematical software like Maple or Mathematica.

2.5 Results and Discussion

This section concerns with the numerical simulation of the channel capacity under suboptimal adaptive technique such as truncated channel inversion with fixed rate (C_{TCIFR}) in Generalized-K fading environment. In numerical simulations, the shadowing

parameter, k =1.0931 and 75.11 for heavy shadowing and light shadowing respectively whereas, the fading parameter m =1 and 2 corresponds to Rayleigh and Rician small scale fading, respectively.

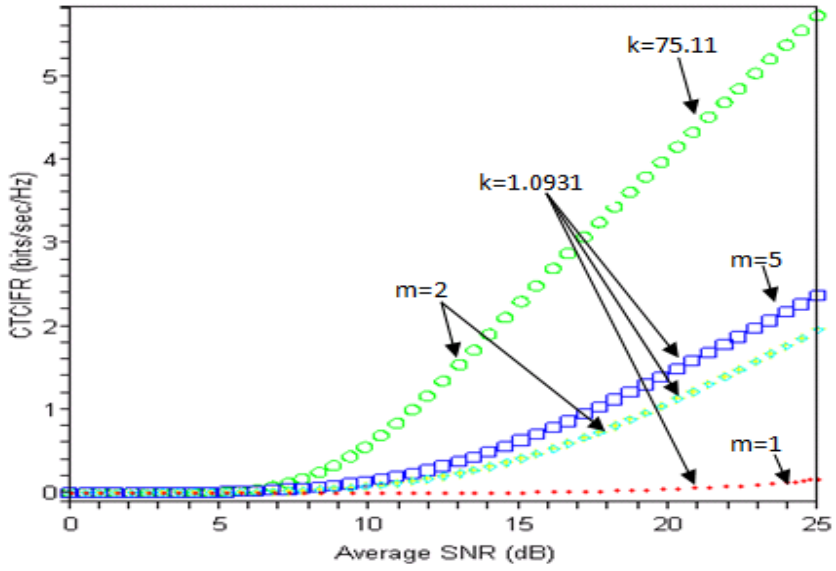

Fig. 2.1 The response of average SNR (dB) over the channel capacity under truncated channel inversion with fixed rate in the Generalized-K fading environment for different fading and shadowing parameters at 10 dB threshold SNR.

Figure 2.1 presents the variation of channel capacity under truncated channel inversion with fixed rate (C_{TCIFR}) per unit bandwidth over Generalized-K fading channel with respect to the average SNR for different levels of fading and shadowing at chosen value of threshold SNR = 10 dB. The threshold SNR refers to the cut off value below which the communication over the channel is not possible and therefore the capacity increases only after the value of average SNR becomes greater than that of the threshold value. As the fading parameter increases (without considering the effect of shadowing), the channel capacity increases with increase of average SNR beyond the threshold value of SNR. However, with the consideration of the effect of shadowing with fading, the channel capacity is much more for light shadowing as compared to that of the heavy shadowing as illustrated in Fig. 2.1.

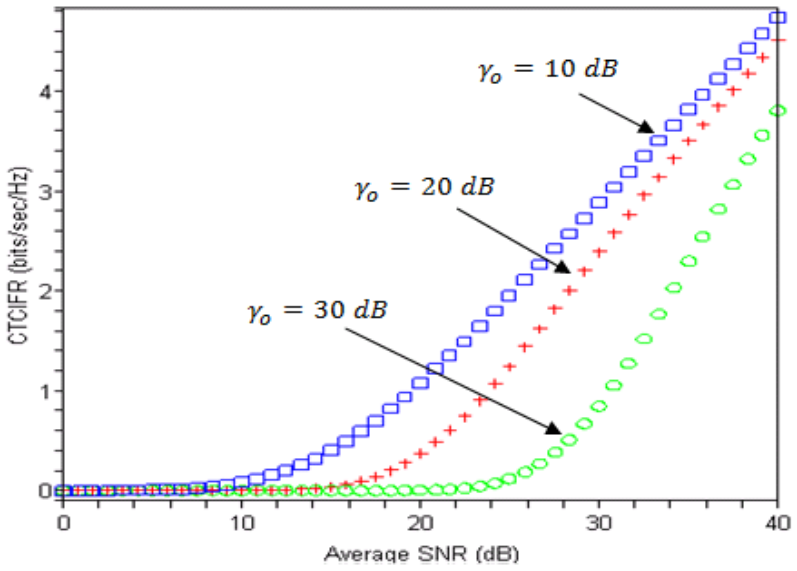

Fig. 2.2 The response of average SNR (dB) over the channel capacity under truncated channel inversion with fixed rate in Generalized-K fading environment for different values of threshold SNR and fixed values of *m* and *k*.

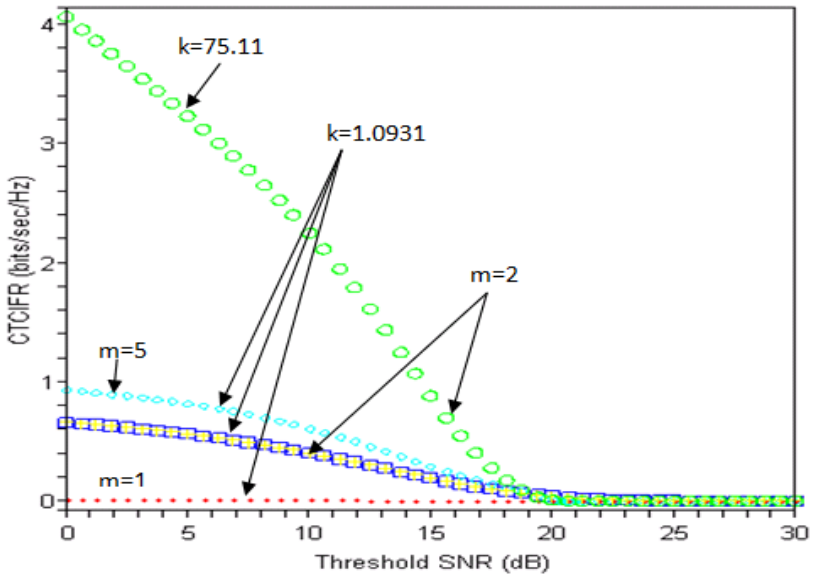

Fig. 2.3 The response of threshold SNR (dB) over the channel capacity under truncated channel inversion with fixed rate in Generalized-K fading environment for different values of fading and shadowing parameters at 15 dB average SNR.

Figure 2.2 shows the channel capacity variation with respect to the average SNR and for different values of threshold SNR at fixed values of fading parameter, m = 2 and shadowing parameter, k = 1.0931. Initially, the channel capacity is approximately zero,

however as the value of average SNR reaches the value of threshold SNR it starts increasing linearly. The channel capacity for truncated channel inversion with fixed rate in Generalized-K fading environment increases with the decrease of the threshold SNR as shown in Fig. 2.2. Figure 2.3 depicts the variation of channel capacity with truncated channel inversion and fixed rate with respect to threshold SNR at chosen value average SNR of 15 dB for several values of multipath fading parameter *m* as well as shadowing parameter *k*. The channel capacity decreases with increase in the value of threshold SNR and becomes zero as the value of threshold SNR exceeds the value of average SNR. Figure 2.4 illustrates the characteristic of channel capacity with threshold SNR for different values of average SNR with chosen values of fading and shadowing parameter such as m =2 and k = 1.0931. However, the channel capacity increases significantly with increase in the average SNR. In addition to this rate of increase of the truncated channel capacity with fixed rate at higher value of average SNR is more as compared to that of the lower values of average SNR for fixed threshold value.

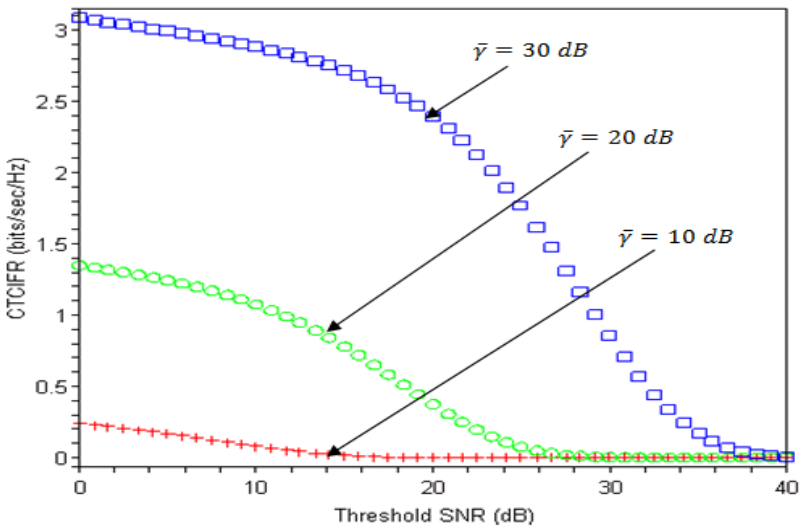

Fig. 2.4 The response of threshold SNR (dB) over the channel capacity under truncated channel inversion with fixed rate in Generalized-K fading environment for different values of average SNR and fixed values of *m* and *k*.

We have validated the MMGF based approach for channel capacity under channel inversion with fixed rate (C_{CIFR}) with reported PDF based [100] and MGF based [96] approaches, which are comparable as shown in Fig. 2.5. Figure 2.5 depicts the variation

of channel capacity under channel inversion with fixed rate with respect to the average SNR with chosen values of m = 2 and k = 75.11 for different approaches.

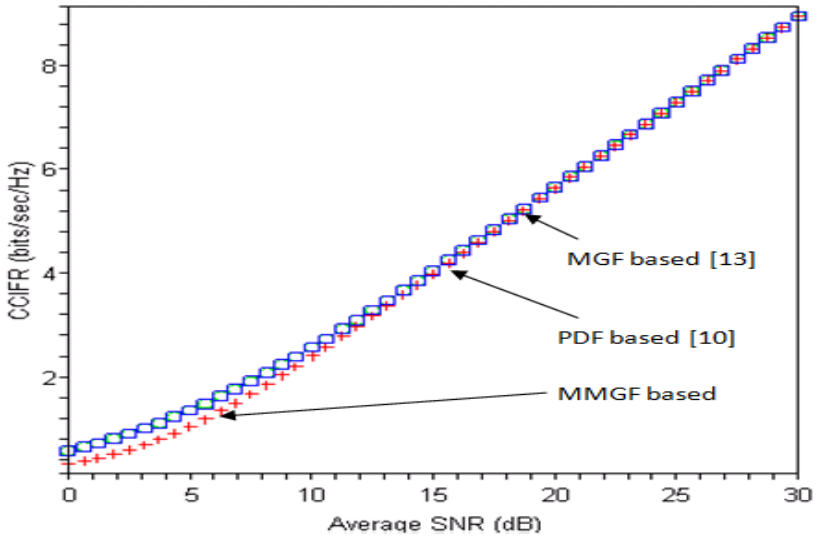

Fig. 2.5 The response of average SNR (dB) over the channel capacity under channel inversion with fixed rate in Generalized-K fading environment with various approaches for m = 2 and k = 75.11

2.6 Summary

In this chapter, we have presented MMGF based channel capacity analysis for suboptimal adaptation technique for Generalized-K fading channel where the power is adapted in accordance to channel state information with fixed transmission rate which is simple and novel approach. The perfect channel state information is assumed to be available at the transmitter so that it can adapt in accordance to the channel state. We have derived analytical expressions for the channel capacity under channel inversion with fixed rate (C_{CIFR}) and for the truncated channel inversion with fixed rate (C_{TCIFR}), which is valid for arbitrary values of the shaping parameters k and m and where, k-m is not an integer and analysis over that expression is performed.

CHAPTER 3

CHANNEL CAPACITY AND OUTAGE PROBABILITY ANALYSIS FOR DISTRIBUTED ANTENNA SYSTEM

3.1 Introduction

Recently, to improve the usage of radio resources and to have larger coverage range for wireless communication systems, the distributed communication system is an emerging technology in which the antennas are distributed throughout the cell and are attached to the base station (BS), simultaneously serving a mobile station (MS). This system reduces the distance of transmission from BS to MS and consequently, reducing the required energy consumption of the systems. However, such a distributed system is known as distributed antenna system (DAS), where the distributed ports are known as relay nodes (RN) and are designed in order to improve the cell edge throughput. The relaying techniques in distributed communication systems are classified as transparent relaying/non regenerative relaying technique and regenerative relaying technique. The transparent relaying does not modify the information or signal received or may allow simple amplification and/or phase rotations. It includes amplify and forward relaying, linear process and forward relaying and non-linear process and forward relaying. In contrast, the regenerative relaying technique as the name indicates, modify the received information or signal and thus require signaling mechanisms and complex operations. It includes decode and forward, estimate and forward and compress and forward relaying techniques [29-31]. The relay communication increases the network capacity by efficiently distributing the resources throughout the cell and improves the coverage area [97- 100]. However, we can have single and multiple relay nodes in between the BS and MS. The multiple relay nodes can be operated with multiple hops, where the nodes are connected in series and with dual hop, where the nodes are connected in parallel in order to have improvement over the path loss gain and diversity gain, respectively [29]. The

optimization over deployment of relay nodes is considered by using the relay site planning (RSP) in order to have an optimum performance level [101]. However, for simplification of simulation, the arbitrary position for RN is considered in this paper. Depending upon the flexibility of RN, they can be classified as fixed or mobile relays. The fixed relay have low cost and fixed radio infrastructure with smaller transmission power and coverage area as compared to the BS. They store the data received from the BS and forwards it to the MS and vice versa [32, 33]. DAS along with its benefits pose some disadvantages such as additional delays introduced in relaying process, fast signaling, time synchronization and increased interference. However, advantages overweigh these cons; thus, form DAS as the future technology for wireless communication.

The distributed communication between RN and MS has lead to the significance of considering composite fading models for the wireless channel. Since, the distance from distributed antennas to the MS is different, the path loss must be considered in fading model. Also, the DAs are separated by large distances and therefore have different levels of shadowing and therefore, considering only the small scale fading models such as Rayleigh, Rician or Nakagami would not be sufficient to model the wireless channels for DAs and it would result in inaccurate channel approximation. The practical scenarios for distributed communication systems has motivated for a composite fading model incorporating effects of path loss, shadowing and fading simultaneously. The multipath fading is often modeled by Rayleigh, Rician or Nakagami-m distribution; the shadowing is modeled by using Log-normal distribution or Gamma distribution and path loss by the generalized Friis equation [1- 4]. Nikolopoulos et al. [14] have investigated narrow band in indoor DAS, by considering only the fast fading. The Rayleigh and Nakagami-m are special cases of the generalized Gamma distribution [58] and thus the composite fading model can be generalized by using this distribution. Therefore, we have performed the channel capacity and outage probability analysis for DAS with fixed and transparent relays over the composite fading channel model using the joint distribution of generalized Gamma, lognormal and path loss distribution.

In this chapter, we have derived analytical expressions for the outage probability and the downlink channel capacity for composite fading environment between DA and MS.

However, the numerically simulated results have been provided for transmission with single relay node as well as with multiple relay nodes between the transmitter and the receiver.

3.2 System Model

In the proposed system model, a single cell is considered with N number of distributed antennas/relay nodes at arbitrary locations within the coverage of cell. The DAS are denoted as DAi (i = 1,2,3,…..N). The transparent relaying technique is considered with the fixed relay nodes, that is, simply forward the coming signal or information to the destination. The positions of DAs and MS are denoted by polar coordinates (ρ, θ) and$(Di, \theta i)$, respectively and are taken from the cell centre, where BS is assumed to be located. Figure 1 shows the distributed antenna system with N number of relay nodes and centrally located BS.

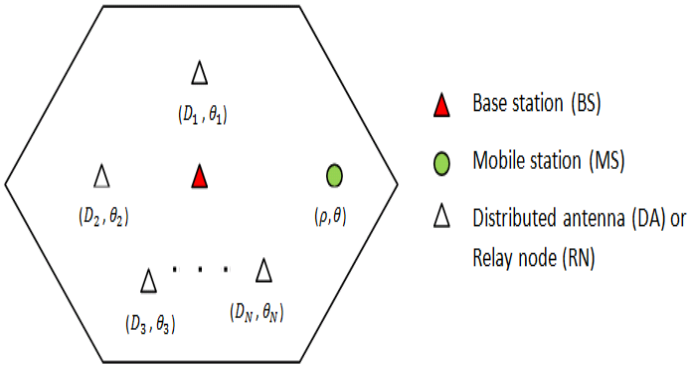

Fig.3.1 The proposed Distributed antenna system (DAS) with N number of relay nodes per cell.

3.3 Channel Model

In the proposed channel model, downlink transmission is considered for the aforementioned system model. Let, h_i represents the channel response between DAi and MS. The composite fading channel model is given as [101]:

$$h_i = G_i\sqrt{L_i(\rho, \theta)\Omega_i} \quad , \forall\, i \in \{1,2 \ldots \ldots N\} \tag{3.1}$$

where, G_i represents the multipath fading between the DA_i and the MS and is modeled by the generalized Gamma distribution as [58]:

$$f_{|G_i|}(g) = \frac{2v_i {m_i}^{m_i} g^{2m_i v_i - 1}}{\Gamma(m_i)} \, exp(-m_i g^{2v_i}) \tag{3.2}$$

where, $m_i \geq 1/2$ is the fading parameter and represents Gaussian, Rayleigh and Rician fading channel for 0.5,1 and 2 respectively and $v_i > 0$ is the shape parameter. $L_i(\rho, \theta)$ denotes the path loss between the DA_i and MS and is derived as [2]:

$$L_i(\rho, \theta) = \left(\frac{d_0}{d_i(\rho,\theta)}\right)^{\beta_i} \tag{3.3}$$

where, d_0 is the reference distance, β_i is the path loss exponent and $d_i(\rho, \theta)$ denotes the distance between DA_i and MS and is expressed as:

$$d_i(\rho, \theta) = \sqrt{\rho^2 + {D_i}^2 - 2\rho D_i \, \cos(\theta - \theta_i)} \tag{3.4}$$

Ω_i represents the shadowing and is modeled by using lognormal distribution as [11]:

$$f_{\Omega_i}(w) = \frac{\xi}{\sqrt{2\pi}\,\sigma_i w} \, exp\left[\frac{-(10log_{10}w - \mu_i)^2}{2{\sigma_i}^2}\right], \qquad w > 0 \tag{3.5}$$

where, $\xi = \frac{10}{\ln(10)}$, μ_i and σ_i are the mean and standard deviation of $10log_{10}w$ .The value for the standard deviation in dB for macrocells and microcells range from 5 to 12 dB and 4 to 13 dB respectively [20]. The output SNR at MS from DA_i can be obtained as:

$$\gamma_i = \frac{E\,|h_i|^2}{N_0} = \frac{E L_i(\rho,\theta)\Omega_i\,|G_i|^2}{N_0} \tag{3.6}$$

The PDF of γ_i is computed in [102] and is expressed as:

$$f_{\gamma_i}(r) = \int_0^\infty f_{\gamma_i/s_i}(r/s)\, f_{s_i}(s) ds$$

$$= \int_0^\infty \frac{v_i {m_i}^{m_i}\, r^{m_i v_i - 1}}{s^{m_i v_i}\,\Gamma(m_i)} \, exp\left[-m_i\left(\frac{r}{s}\right)^{v_i}\right] \frac{\xi}{\sqrt{2\pi}\,\sigma_i s} \, exp\left[\frac{-(10log_{10}s - \tilde{\mu}_i(\rho,\theta))^2}{2{\sigma_i}^2}\right] ds \tag{3.7}$$

where, $\tilde{\mu}_i(\rho, \theta) = \mu_i + 10log_{10}[E\, L_i(\rho, \theta)\, /N_0]$

3.4 Outage Probability and Capacity Analysis

The outage probability is the probability that the received SNR falls below a certain threshold value of SNR [11] and is mathematically defined as:

$$P_{out} = P(\gamma < \gamma_o) \tag{3.8}$$

where, γ is the average received SNR and γ_o is the threshold value of SNR, below which the communication is not possible. The outage probability between the DA_i and the MS is expressed as given by Cai et al in [102] as,

$$P(\gamma_i < \gamma_o) = 1 - \int_{\gamma_o}^{\infty} f_{\gamma_i}(r)\, dr \tag{3.9}$$

$$\cong 1 - \frac{\sum_{n=1}^{N_p} H_n\, \Gamma\left(m_i, m_i\left(\frac{\gamma_o}{10^{\left(\frac{\sqrt{2}\sigma_i\, t_n + \tilde{\mu}_i(\rho,\theta)}{10}\right)}}\right)^{v_i}\right)}{\sqrt{\pi}\, \Gamma(m_i)} \tag{3.10}$$

where, t_n and H_n are the base points and weight factors of the N_p order Hermite polynomial, respectively. The above expression for outage probability represents the outage in a single link, when the selection combining is considered. In order to represent the outage probability for the complete system with N number of relaying nodes and with the assumption that each link is assumed to be independent, the total outage probability is the product of outage probabilities of individual link [102]. Thus, the outage probability for optimum combining at the receiver is expressed as:

$$P(\gamma < \gamma_o) \cong \prod_{i=1}^{N} \left[1 - \frac{\sum_{n=1}^{N_p} H_n\, \Gamma\left(m_i, m_i\left(\frac{\gamma_o}{10^{\left(\frac{\sqrt{2}\sigma_i\, t_n + \tilde{\mu}_i(\rho,\theta)}{10}\right)}}\right)^{v_i}\right)}{\sqrt{\pi}\, \Gamma(m_i)} \right] \tag{3.11}$$

The channel capacity for DA_i with composite fading environment (path loss, shadowing and multipath fading effects) is given as:

$$C_i = \int_0^{\infty} \ln(1 + r)\, f_{\gamma_i}(r)\, dr \tag{3.12}$$

By putting the value of $f_{\gamma_i}(r)$ from eq. (3.7) into eq. (3.12) we have,

$$C_i = \int_0^\infty \ln(1+r) \int_0^\infty \frac{v_i {m_i}^{m_i} r^{m_i v_i - 1}}{s^{m_i v_i}\, \Gamma(m_i)} \; exp\left[-m_i \left(\frac{r}{s}\right)^{v_i}\right] \frac{\xi}{\sqrt{2\pi}\,\sigma_i s} \; exp\left[\frac{-(10log_{10}s - \tilde{\mu}_i(\rho,\theta))^2}{2{\sigma_i}^2}\right] ds\, dr \tag{3.13}$$

For the simplification of expression, let us consider the value of shape parameter to be unity. Thus,

$$C_i = \int_0^\infty \ln(1+r) \int_0^\infty \frac{{m_i}^{m_i} r^{m_i - 1}}{s^{m_i}\, \Gamma(m_i)} \; exp\left[-m_i \frac{r}{s}\right] \frac{\xi}{\sqrt{2\pi}\,\sigma_i s} \; exp\left[\frac{-(10log_{10}s - \tilde{\mu}_i(\rho,\theta))^2}{2{\sigma_i}^2}\right] ds\, dr$$

$$= \int_0^\infty \frac{\xi}{\sqrt{2\pi}\,\sigma_i s} \; exp\left[\frac{-(10log_{10}s - \tilde{\mu}_i(\rho,\theta))^2}{2{\sigma_i}^2}\right] \frac{{m_i}^{m_i}}{s^{m_i}\, \Gamma(m_i)} \int_0^\infty \ln(1+r)\, r^{m_i - 1} exp\left[-m_i \frac{r}{s}\right] dr\, ds \tag{3.14}$$

Let, $I_1 = \int_0^\infty \ln(1+r)\, r^{m_i - 1} exp\left[-m_i \frac{r}{s}\right] dr$ (3.15)

Using the identity [11, 103],

$$\int_0^\infty \ln(1+x)\, x^{n-1} exp(-\mu x) dx = (n-1)!\; exp(\mu) \sum_{k=1}^{n} \frac{\Gamma(k-n, \mu)}{\mu^k}$$

The Eq. (3.15) is written as,

$$I_1 = (m_i - 1)!\; exp\left(\frac{m_i}{s}\right) \sum_{k=1}^{m_i} \frac{\Gamma(k-m_i, m_i/s)}{\left(\frac{m_i}{s}\right)^k} \tag{3.16}$$

By replacing the integral in eq. (3.14) by using eq. (3.16), we have

$$C_i = \int_0^\infty \frac{\xi}{\sqrt{2\pi}\,\sigma_i s} \; exp\left[\frac{-(10log_{10}s - \tilde{\mu}_i(\rho,\theta))^2}{2{\sigma_i}^2}\right] \frac{{m_i}^{m_i}}{s^{m_i}\, \Gamma(m_i)} (m_i - 1)!\, exp\left(\frac{m_i}{s}\right) \sum_{k=1}^{m_i} \frac{\Gamma(k-m_i, m_i/s)}{\left(\frac{m_i}{s}\right)^k} ds$$

$$C_i = \int_0^\infty \frac{\xi}{\sqrt{2\pi}\,\sigma_i s} \; exp\left[\frac{-(10log_{10}s - \tilde{\mu}_i(\rho,\theta))^2}{2{\sigma_i}^2}\right] \frac{{m_i}^{m_i} \Gamma(m_i)}{s^{m_i}\, \Gamma(m_i)} \; exp\left(\frac{m_i}{s}\right) \sum_{k=1}^{m_i} \frac{\Gamma(k-m_i, m_i/s)}{\left(\frac{m_i}{s}\right)^k} ds$$

By changing the order of integration and summation we have,

$$C_i = \sum_{k=1}^{m_i} \int_0^{\infty} \frac{\xi}{\sqrt{2\pi}\,\sigma_i s}\; exp\left[\frac{-(10log_{10}s-\tilde{\mu}_i(\rho,\theta))^2}{2{\sigma_i}^2}\right] \frac{{m_i}^{m_i}}{s^{m_i}} exp\left(\frac{m_i}{s}\right) \frac{\Gamma(k-m_i,m_i/s)}{\left(\frac{m_i}{s}\right)^k}\; ds$$

$$= \sum_{k=1}^{m_i} \frac{\xi\; {m_i}^{m_i-k}}{\sqrt{2\pi}\,\sigma_i} \int_0^{\infty} exp\left[\frac{-(10log_{10}s-\tilde{\mu}_i(\rho,\theta))^2}{2{\sigma_i}^2}\right] exp\left(\frac{m_i}{s}\right)\; s^{k-m_i-1}\; \Gamma(k-m_i,m_i/s)ds$$

(3.17)

Now, let $\frac{10log_{10}s-\tilde{\mu}_i(\rho,\theta)}{\sqrt{2}\sigma_i} = x$

Thus, by change of the variables eq. (3.17) becomes,

$$C_i = \sum_{k=1}^{m_i} \frac{{m_i}^{m_i-k}}{\sqrt{\pi}} \int_{-\infty}^{\infty} exp[-x^2]\, exp\left(\frac{m_i}{10^{\left(\frac{\sqrt{2}\sigma_i x+\tilde{\mu}_i(\rho,\theta)}{10}\right)}}\right) \left(10^{\left(\frac{\sqrt{2}\sigma_i x+\tilde{\mu}_i(\rho,\theta)}{10}\right)}\right)^{k-m_i}\; \Gamma\left(k-\right.$$

$$\left. m_i, m_i/10^{\left(\frac{\sqrt{2}\sigma_i x+\tilde{\mu}_i(\rho,\theta)}{10}\right)}\right) dx \qquad (3.18)$$

Using Gauss-Hermite integration [14, Eq. (25, 4, 46)] as:

$$\int_{-\infty}^{\infty} exp[-x^2]\, f(x)dx \cong \sum_{p=1}^{N_p} H_n\, f(t_n)$$

where, t_n and H_n are the base points and the weight factors of the N_p order Hermite polynomial. Thus, eq. (3.18) reduces to the following capacity expression for DA_i as:

$$C_i = \sum_{k=1}^{m_i} \frac{{m_i}^{m_i-k}}{\sqrt{\pi}} \sum_{p=1}^{N_p} H_n\; exp\left(\frac{m_i}{10^{\left(\frac{\sqrt{2}\sigma_i\, t_n+\tilde{\mu}_i(\rho,\theta)}{10}\right)}}\right) \left(10^{\left(\frac{\sqrt{2}\sigma_i\, t_n+\tilde{\mu}_i(\rho,\theta)}{10}\right)}\right)^{k-m_i}\; \Gamma\left(k-\right.$$

$$\left. m_i, m_i/10^{\left(\frac{\sqrt{2}\sigma_i\, t_n+\tilde{\mu}_i(\rho,\theta)}{10}\right)}\right) \qquad (3.19)$$

The equivalent capacity of the system for two different scenarios is given as:

1. Single node relaying

For single node relaying, total system capacity would be the capacity of the link between the DA_i and the MS and is given as:

$$C_{system} = C_i \tag{3.20}$$

2. Multiple node relaying

For transmission through multiple relay nodes, the total system capacity would be equal to the sum of individual capacities of distributed antennas. For such a technique and with N total number of distributed antennas, the equivalent capacity would become:

$$C_{system} = \sum_{i=1}^{N} \sum_{k=1}^{m_i} \frac{{m_i}^{m_i - k}}{\sqrt{\pi}} \sum_{p=1}^{N_p} H_n \; exp\left(\frac{m_i}{10^{\left(\frac{\sqrt{2}\sigma_i \, t_n + \tilde{\mu}_i(\rho,\theta)}{10}\right)}} \right) \left(10^{\left(\frac{\sqrt{2}\sigma_i \, t_n + \tilde{\mu}_i(\rho,\theta)}{10}\right)} \right)^{k - m_i} \Gamma\left(k - m_i, m_i / 10^{\left(\frac{\sqrt{2}\sigma_i \, t_n + \tilde{\mu}_i(\rho,\theta)}{10}\right)} \right) \tag{3.21}$$

3.5 Simulation Parameters

We have considered that the fading parameters along all the wireless links between DAi and MS are similar in the proposed system model. However, various values of fading parameters for each link can be taken for exact evaluation. The list of simulation parameters are shown in the Table 1.

Table 1. Numerical values of the simulation parameters for capacity analysis with respect to average SNR.

Parameters	**Symbol**	**Value**
Path loss exponent	β	0,2,3
Number of distributed antennas	N	3
Mean of shadow fading	μ	0 dB
Standard deviation of shadow fading	σ	8 dB
Fading parameter	m	1, 2
Shape parameter	v	1
Order of Hermite polynomial	N_p	4

3.6 Results and Discussion

This section concerns with the simulation results for outage probability and channel capacity of DAS with aforementioned simulation parameters. We have considered transparent relaying technique with fixed relay nodes. The analytical expression has been derived for channel capacity using Gauss Hermite Quadrature approximation. The response of average SNR over the outage probability are shown in Fig.3.2 (a) and Fig.3.2 (b) for single node relaying and multiple node relaying respectively for different values of fading parameter *m* with value of path loss exponent equal to 2, zero dB mean and 8 dB standard deviation of the shadowing distribution. The outage performance improves with the increasing values of fading parameter *m* as illustrated by the Fig.2.. For the Gaussian fading channel (*m* = 0.5), the outage is having worst response and improves for Rayleigh (*m* = 1) and Rician (*m* = 2) fading channels. In case of the multiple node relaying, where all the links are considered to be independent, the total outage probability for the system has better response as compared to that of the selection combining. For instance, outage probability with *m*=2 (Rician fading channel) is zero at nearly 44 dB of average received SNR in case of optimum combining, whereas, the average received SNR of approximately 55 dB is required for the outage probability to be zero for the single node relaying techniques. Thus, a large penalty over the average received SNR is mitigated by using DAS with a number of relaying nodes communicating with the MS.

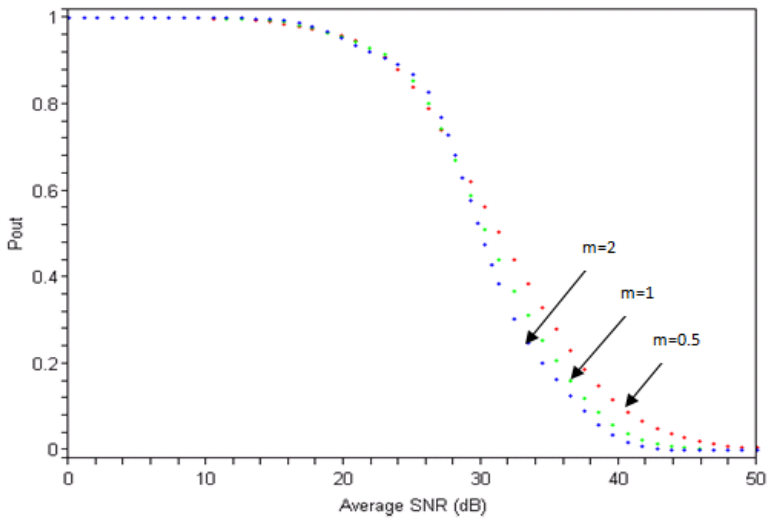

(a)

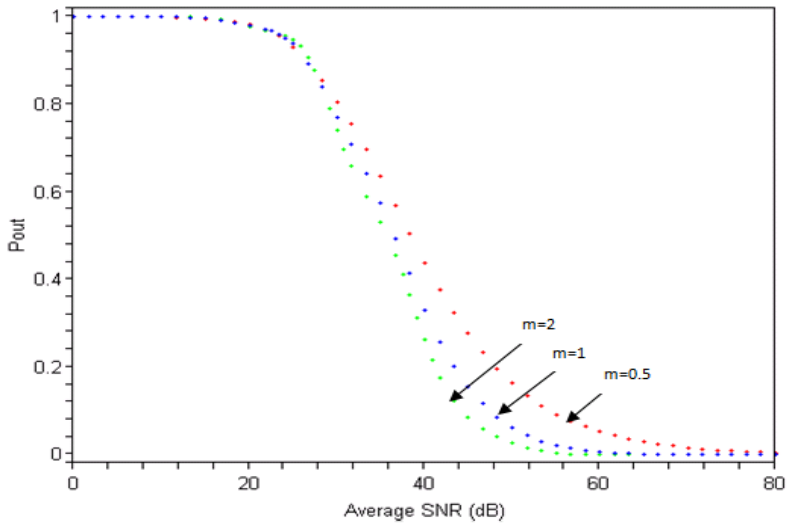

(b)

Fig. 3.2 The average SNR response over the outage probability with respect to different values of fading parameter (m = 0.5, 1 and 2) for a) multiple node relaying and b) single node relaying techniques.

The variation of outage probability with respect to the average SNR for different values of threshold SNR with fading parameter m = 1, path loss exponent, $\beta = 2$ and zero dB mean and 8 dB standard deviation of shadowing distribution is shown in Fig.3.3, which reveals that when the value of threshold SNR is greater than the value of average received SNR, there is a no communication possible and system is said to be in outage and therefore, the outage probability is maximum that is unity. As the value of received SNR increases beyond the threshold SNR, the outage probability tends to decrease and becomes zero. In addition to this, the outage performance improves with the lower values of threshold SNR and increasing values of average received SNR.

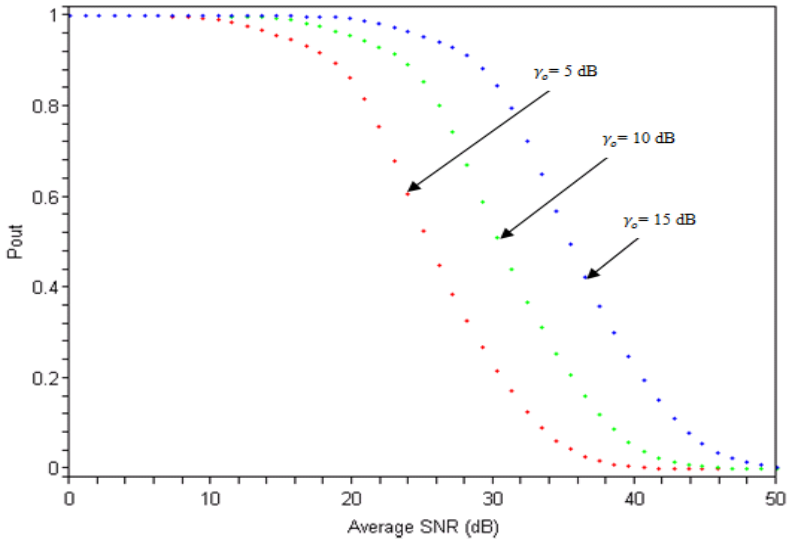

Fig. 3.3 The average SNR response over the outage probability with respect to different values of threshold SNR and fixed values of fading parameters.

The channel capacity variation with respect to the average received SNR are shown in Fig. 3.4 The channel capacity response with respect to average SNR for different values of fading parameter m = 1 and 5 for multiple node relaying and single node relaying are shown in Fig. 3.4 (a) and Fig.3.4 (b) respectively. However, the other parameters are kept constant, that is, path loss exponent (2), zero dB mean and 8 dB standard deviation of the shadowing distribution. The channel capacity improves with the increasing value of fading parameter m as well as with the number of relaying links. The channel capacity variation with respect to average SNR for different values of path loss exponent under multiple node and single node relaying techniques are shown in Fig. 3.5(a) and Fig. 3.5(b), respectively. The channel capacity improves with the decreasing values of path loss exponent and clearly for $\beta = 0$ (when path loss is not considered), we have maximum channel capacity with fixed value of fading parameter m = 1 and zero dB mean and 8 dB standard deviation of shadowing distribution.

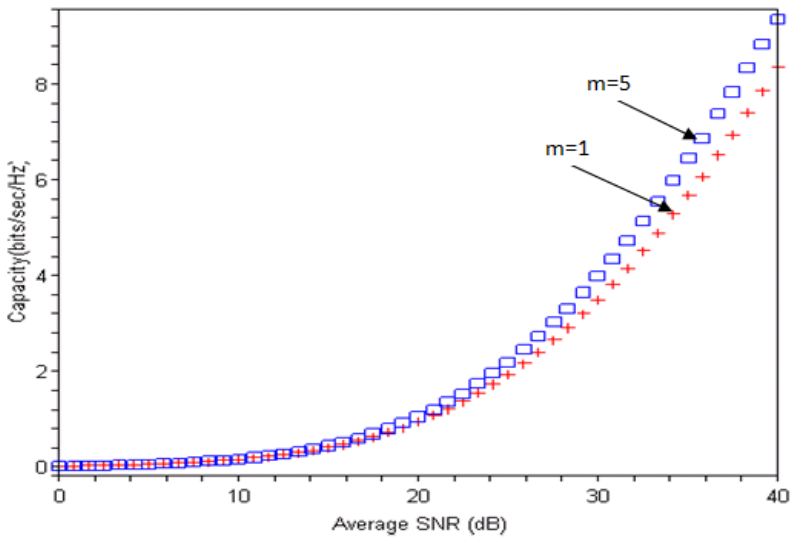

(a)

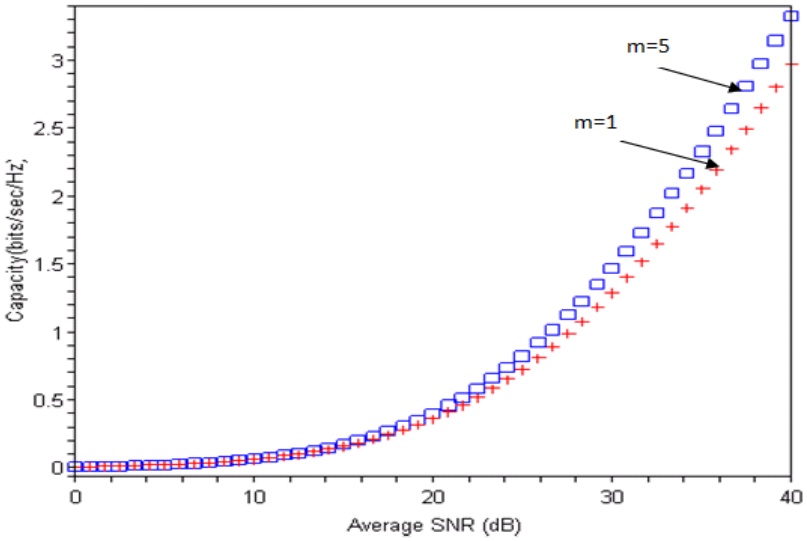

(b)

Fig. 3.4 The channel capacity variation with respect to the average SNR for different values of fading parameter m for a) multiple node and b) single node relaying techniques.

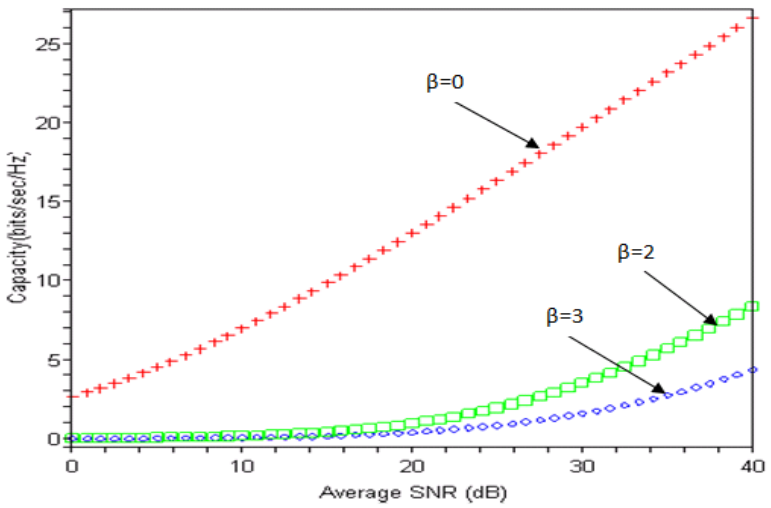

(a)

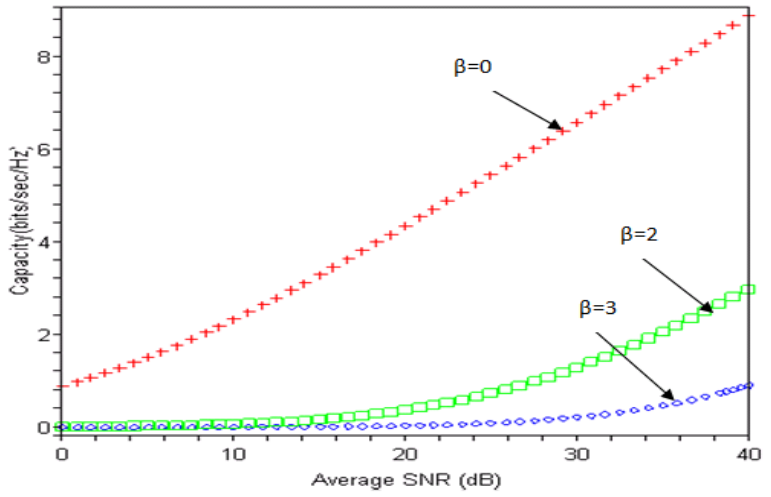

(b)

Fig. 3.5 The channel capacity variation with respect to the average SNR for different values of path loss exponent $\boldsymbol{\beta}$ for a) multiple node and b) single node relaying.

3.6 Summary

In this chapter, a system model of DAS with transparent relaying technique and fixed relay nodes is considered over composite fading environment and numerical analysis is provided. The analytical expressions using numerical approximation has been derived for the outage probability and channel capacity for single node relaying and multiple node

relaying techniques for the proposed system model. The simulation results have been shown to validate the performance improvement with the use of DAS, and much closer approximation to practical scenario is provided by considering the combined effect of various types of fading in a more generalized form.

CHAPTER 4

THE ADAPTIVE CHANNEL CAPACITY USING MRC COMBINING OVER GENERALIZED-K FADING CHANNEL

4.1 Introduction

The wireless communication channel in contrast to the wireline channel is highly indeterministic and is often prone to low received signal power. The random variation in received signal strength is termed as fading. Signal propagates through the wireless channel with the introduction of path loss, shadowing and multipath/small scale fading [2, 3]. Multipath fading results due to constructive or destructive interference of multiple copies of the transmitted signal when combined at the receiver. These multiple copies of the signal are formed due to various mechanisms such as reflection, diffraction and scattering [2, 4, 11]. Multipath fading is modeled by using Rayleigh, Rician or Nakagami distribution and shadowing by using lognormal distribution [7]. However, practical scenarios show that the multipath fading and shadowing occur simultaneously and therefore a composite fading model is considered for the analysis. The composite fading models comprising of lognormal distribution fail to provide closed form expressions and may result into complex integrals. Thus, the most accurate approximation to the composite fading environment is provided by Generalized-K distribution, where, lognormal distribution is replaced by a simpler approximate that is, Gamma distribution.

The simplest way to mitigate the effect of channel fading is to employ diversity technique [104, 11]. The diversity techniques are used to compensate for fading impairments without the use of training sequence and therefore, reduce the overhead as compared to the equalization techniques [3]. The implementation of diversity combining technique requires two or more antennas at the receiver and can be employed both at the BS and mobile receivers. The various ways to exploit diversity at the BS are: 1) Spatial diversity, where multiple antenna elements are used to provide diversity gains. 2) Frequency

diversity, where the signal is transmitted over several carriers and 3) Time diversity, where the signal is transmitted in different time slots to provide diversity benefit. The various diversity combining techniques at receiver can be categorized as: Selection combining (SC), Equal gain combining (EGC), Maximal ratio combining (MRC) and Switch and stay combining techniques (SSC) [11].

The performance analysis over diversity combining techniques for fading channels has been reported in literature. In [25], Ricean and Suzuki distributions were used to model the land-mobile satellite channel and performance evaluation of M-ary phase shift keying (PSK) and M-ary differential phase shift keying (DPSK) using micro-diversity reception technique was studied for SC and MRC. Gaber et al [63], have provided outage probability analysis for cooperative diversity wireless networks using amplify and forward relays over independent and not identically distributed weibull and Weibull-Lognormal for single and multiple relays. Yilmaz and Alouini [85], has computed average channel capacity under an unified framework for two diversity combining techniques namely Equal Gain Combining (EGC) and maximal ratio combining (MRC) and has derived a novel closed form expression for MGF for Generalized k fading. In [104], expression for the outage probability of dual branch SC over generalized Gamma fading channel has been provided. In this chapter we provide closed form expression for channel capacity under truncated channel inversion with fixed rate over Generalized-K fading environment and MRC combining technique at the receiver.

4.2 Generalized-K Fading Channel Model for MRC

The Generalized-K distribution is the joint distribution of Nakagami-*m* and Gamma distribution which are used to model the multipath fading and shadowing, respectively. However, it is the most generalized case as it can model various fading levels by a sheer change in its shaping parameters. The PDF of received SNR over the Generalized-K distribution is given as [71]:

$$f_\gamma(\gamma) = \frac{2\Xi^{\frac{(\beta+1)}{2}}\gamma^{\frac{(\beta-1)}{2}}}{\Gamma(m)\Gamma(k)} K_\alpha\left(2\sqrt{\Xi\gamma}\right) \qquad \gamma \geq 0 \tag{4.1}$$

where, $\Xi = \frac{km}{\bar{\gamma}}$, $\alpha = k - m$ and $\beta = k + m - 1$. $\bar{\gamma}$ is the average received SNR, k and m are the shadowing and fading parameters, respectively. $K_\alpha(.)$ is the modified Bessel function of second kind of order α and $\Gamma(.)$ is the gamma function. The instantaneous SNR for L branch MRC diversity system is given as [89]

$$\gamma = \sum_{i=1}^{L} \gamma_i \tag{4.2}$$

The fading level is assumed to be same over all L diversity branches. The PDF of instantaneous SNR at the output of a maximal ratio combiner with L identical branches is obtained by substituting m with Lm and average SNR with increase of factor L in Eq. (4.1) as given in [81].

$$f_\gamma(\gamma) = \frac{2\Xi^{\frac{(\beta+1)}{2}} \gamma^{\frac{(\beta-1)}{2}}}{\Gamma(mL)\Gamma(k)} K_\alpha\left(2\sqrt{\Xi\gamma}\right) \qquad \gamma \geq 0 \tag{4.3}$$

where, $\alpha = k - mL$ and $\beta = k + mL - 1$. For the diversity branches, it is assumed that the distance is very small between the branches and therefore, the shadowing variation is assumed to be constant.

4.3 Marginal Moment Generating Function

However, most framework described for the analysis of spectral efficiency over fading channels in various literature make use of the so-called PDF based approach of the received SNR, which is a task that might be very cumbersome for system setups and often require to manage mathematical expressions. It is also well known fact that the prior knowledge of the CSI at the transmitter is exploited to improve the channel capacity. In this section, MMGF with MRC combining technique is evaluated for Generalized-K fading and further, it is used for computation of the channel capacity. The moment generating function is closely related to the Laplace transform and is given as expectation of $e^{s\gamma}$ and when this expectation is taken above a certain cut off value; we have marginal moment generating function, defined as [69]:

$$\widehat{M}(-s, a) = \int_a^\infty e^{-s\gamma} f_\gamma(\gamma)\, d\gamma \tag{4.4}$$

After substituting the value of $f_\gamma(\gamma)$ from Eq.(4.3), we get:

$$\widehat{M}(-s,\gamma_o) = \int_{\gamma_o}^{\infty} e^{-s\gamma} \frac{2\Xi^{\frac{(\beta+1)}{2}} \gamma^{\frac{(\beta-1)}{2}}}{\Gamma(mL)\Gamma(k)} K_{\alpha}\left(2\sqrt{\Xi\gamma}\right) d\gamma \tag{4.5}$$

By following the similar steps as in chapter 2 for the derivation of MMGF we have,

$$\widehat{M}(-s,\gamma_o)$$
$$= \frac{\pi \csc(\alpha\pi)}{\Gamma(mL)\Gamma(k)} \left\{ \sum_{p=0}^{\infty} \frac{1}{\Gamma(p-\alpha+1)p!} \left(\Xi/s\right)^{\frac{\beta-\alpha+2p+1}{2}} \Gamma\left(\frac{\beta-\alpha+2p+1}{2}, s\gamma_o\right) - \right.$$
$$\left. \sum_{p=0}^{\infty} \frac{1}{\Gamma(p+\alpha+1)p!} \left(\Xi/s\right)^{\frac{\beta+\alpha+2p+1}{2}} \Gamma\left(\frac{\beta+\alpha+2p+1}{2}, s\gamma_o\right) \right\} \tag{4.6}$$

This provides the required mathematical expression for MMGF of Generalized-K fading for MRC combining technique at the receiver.

4.4 Channel Capacity Analysis

The channel capacity has been regarded as the fundamental information theoretic performance measure to predict the maximum information rate of a communication system. It is extensively used as the basic tool for the analysis and design of more efficient techniques to improve the spectral efficiency of the modern wireless communication systems and to gain insight into how to counteract the detrimental effects of the multipath fading propagation via opportunistic and adaptive communication methods. Shannon [85] has evaluated the channel capacity for additive white Gaussian noise (AWGN) channel. However, it cannot be used directly for fading channel, leading to the case of ergodic capacity, which is the average of Shannon's capacity over the distribution of received SNR. This average capacity is improved by using CSI at transmitter, which is made available at transmitter by the receiver through a feedback path. In this analysis, we have considered that the transmitter is having perfect CSI and based on this the transmitter now adapts its transmission rate, power and coding techniques to have various optimal and suboptimal adaptation techniques, namely, C_{ORA}, C_{OPRA}, C_{CIFR} and C_{TCIFR}. In C_{ORA} only the transmission rate is varied in accordance to CSI keeping power constant and for C_{OPRA} both power and rate are varied, simultaneously. In C_{CIFR}, the transmitter adapts its transmission power in such a way that

constant SNR is maintained at the receiver with a fixed transmission rate, that is the channel fading effects are assumed to be inverted. Therefore, the receiver assumes fading channel to be time invariant AWGN channel and if the channel fading effect is inverted above a certain threshold value, then we have channel capacity under truncated channel inversion with fixed rate. The channel capacity for suboptimal adaptation technique in terms of PDF of received SNR is given as [94].

$$C_{TCIFR} = Blog_2\left(1 + \frac{1}{\int_{\gamma_o}^{\infty} \frac{f_\gamma(\gamma)}{\gamma} d\gamma}\right)(1 - P_{out}) \tag{4.7}$$

where, P_{out} = the outage probability and B is the channel bandwidth. By replacing, $\frac{1}{\gamma} = \int_0^{\infty} e^{-s\gamma}\, ds$ and changing the order of integral, we have channel capacity in terms of MMGF as:

$$C_{TCIFR} = Blog_2\left(1 + \frac{1}{\int_0^{\infty} \widehat{M}(-s,\gamma_o) d\gamma}\right)(1 - P_{out}) \tag{4.7}$$

By substituting the value of MMGF from Eq.(4.6) and evaluating the integral as:

$$I = \frac{\pi \csc(\alpha\pi)}{2^{\beta-1}\Gamma(mL)\Gamma(k)}\left[\sum_{p=0}^{\infty} \frac{1}{\Gamma(p-\alpha+1)p!} \Xi^{\frac{\beta-\alpha+2p+1}{2}} I_3 - \sum_{p=0}^{\infty} \frac{1}{\Gamma(p+\alpha+1)p!} \Xi^{\frac{\beta+\alpha+2p+1}{2}} I_4\right] \tag{4.8}$$

where,

$$I_3 = \int_0^{\infty} s^{-\left(\frac{\beta-\alpha+2p+1}{2}\right)} \Gamma\left(\frac{\beta-\alpha+2p+1}{2}, s\gamma_o\right) ds \tag{4.9}$$

and

$$I_4 = \int_0^{\infty} s^{-\left(\frac{\beta+\alpha+2p+1}{2}\right)} \Gamma\left(\frac{\beta+\alpha+2p+1}{2}, s\gamma_o\right) ds \tag{4.10}$$

Using [96, Eq. (8.4.16.2)] and [96, Eq. (2.24.2.1)], we have:

$$I_3 = \gamma_o^{\left(\frac{\beta-\alpha+2p-1}{2}\right)} \frac{\Gamma\left(\frac{1-(\beta-\alpha+2p)}{2}\right)}{\Gamma\left(1+\frac{1-(\beta-\alpha+2p)}{2}\right)} \tag{4.11}$$

and

$$I_4 = \gamma_o^{\left(\frac{\beta+\alpha+2p-1}{2}\right)} \frac{\Gamma\left(\frac{1-(\beta+\alpha+2p)}{2}\right)}{\Gamma\left(1+\frac{1-(\beta+\alpha+2p)}{2}\right)} \tag{4.12}$$

By putting Eq.(4.11) and Eq.(4.12) in Eq.(4.8), we get:

$$I = \frac{\pi \csc(\alpha\pi)}{\Gamma(mL)\Gamma(k)}\left[\sum_{p=0}^{\infty}\frac{\gamma_o^{\left(\frac{\beta-\alpha+2p-1}{2}\right)}}{\Gamma(p-\alpha+1)p!}\Xi^{\frac{\beta-\alpha+2p+1}{2}}\frac{\Gamma\left(\frac{1-(\beta-\alpha+2p)}{2}\right)}{\Gamma\left(1+\frac{1-(\beta-\alpha+2p)}{2}\right)} - \sum_{p=0}^{\infty}\frac{\gamma_o^{\left(\frac{\beta+\alpha+2p-1}{2}\right)}}{\Gamma(p+\alpha+1)p!}\Xi^{\frac{\beta+\alpha+2p+1}{2}}\frac{\Gamma\left(\frac{1-(\beta+\alpha+2p)}{2}\right)}{\Gamma\left(1+\frac{1-(\beta+\alpha+2p)}{2}\right)}\right] \quad (4.13)$$

The outage probability is defined as the probability that the received SNR falls below a certain threshold value and is given as [71, 78]:

$$P_{out} = P(\gamma \leq \gamma_o) \quad (4.14)$$

For L branch diversity combining technique, the outage probability can be expressed as [78],

$$P_{out} = 1 - \frac{(\Xi\gamma_o)^{\frac{(\beta+1)}{2}}}{\Gamma(mL)\Gamma(k)}\, G_{1,3}^{3,0}\left[\Xi\gamma_o, \begin{matrix} (1-\beta)/2 \\ -(1+\beta)/2 \quad \alpha/2 \quad -\alpha/2 \end{matrix}\right] \quad (4.15)$$

By using Eq.(4.15) and Eq.(4.13) in Eq.(4.7), we have achieved the channel capacity under truncated channel inversion with fixed rate over the Generalized-K fading environment with MRC combining technique at the receiver, where the special functions can be easily evaluated by using mathematical software like Maple or Mathematica.

4.5 Results and Discussion

This section concerns with the numerical simulation of the channel capacity under suboptimal adaptive technique such as truncated channel inversion with fixed rate (C_{TCIFR}) in Generalized-K fading environment with MRC diversity combining technique at receiver. In numerical simulations, the shadowing parameter, k =1.0931 and 75.11 for heavy shadowing and light shadowing respectively whereas, the fading parameter m =1 and 2 corresponds to Rayleigh and Rician small scale fading, respectively.

The variation of channel capacity under truncated channel inversion and fixed rate with respect to the average SNR is provided in Fig. 4.1 for different values of diversity

branches L and fixed values of fading parameter (m=2 for Rician fading channel) and shadowing parameter (k=1.0931 for heavily shadowed environment). The channel capacity improves with the increase in number of diversity branches and with the increase in the value of average SNR.

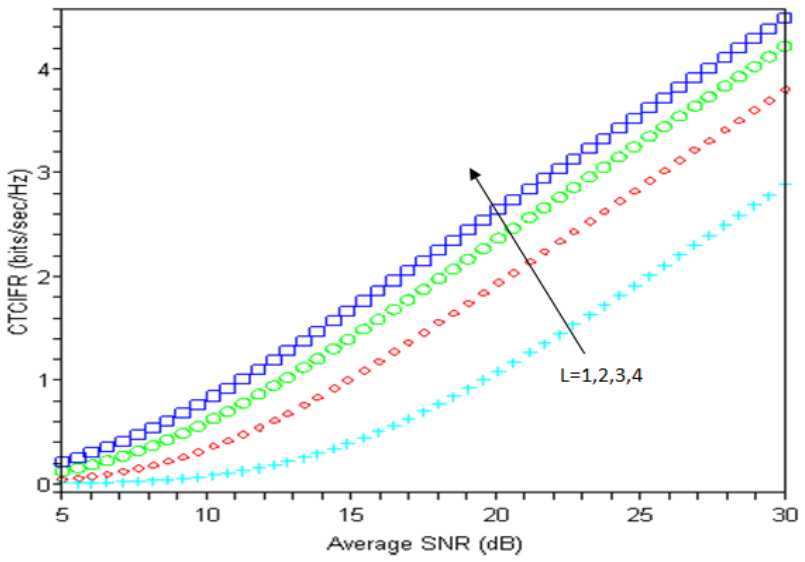

Fig.4.1 The response of channel capacity with truncated channel inversion and fixed rate with respect to average SNR for different values of diversity branches L and fixed values of fading and shadowing parameters (m=2 and k=1.0931).

Figure 4.2 shows the response of channel capacity under truncated channel inversion and fixed for the average SNR with different values of diversity branches and different fade levels (m=1 for Rayleigh fading channel and m=2 for Rician fading channel). The variation for truncated channel inversion and fixed rate channel capacity with respect to the average SNR is shown for two different shadowing scenarios with (a) showing the channel capacity variation in lightly shadowed fading channel and (b) shows the channel capacity variation for heavily shadowed fading channel. The channel capacity improves for the increased values of fading parameter m and with the increased number of diversity branches of MRC combining technique. The increase in channel capacity for light shadowing (k=75.11) is significant as compared to that for the heavily shadowed fading channel (k=1.0931).

Figure 4.3 shows the response of channel capacity of truncated channel inversion and fixed rate with respect to the threshold SNR for different values of fading parameter and

the number of diversity branches with (a) heavy shadowing and (b) light shadowing and with the average SNR of 15 dB. The threshold SNR defines the minimum cut off level for the value of the received SNR below which communication is not possible. Therefore the channel capacity decreases drastically for the greater values of the threshold SNR as compared to the average SNR, because as the value of average SNR falls below to that of the threshold SNR, the communication between the transmitter and the receiver is not possible and therefore, the channel capacity decreases significantly . However, for lower values of the threshold SNR the channel capacity improvement is observed.

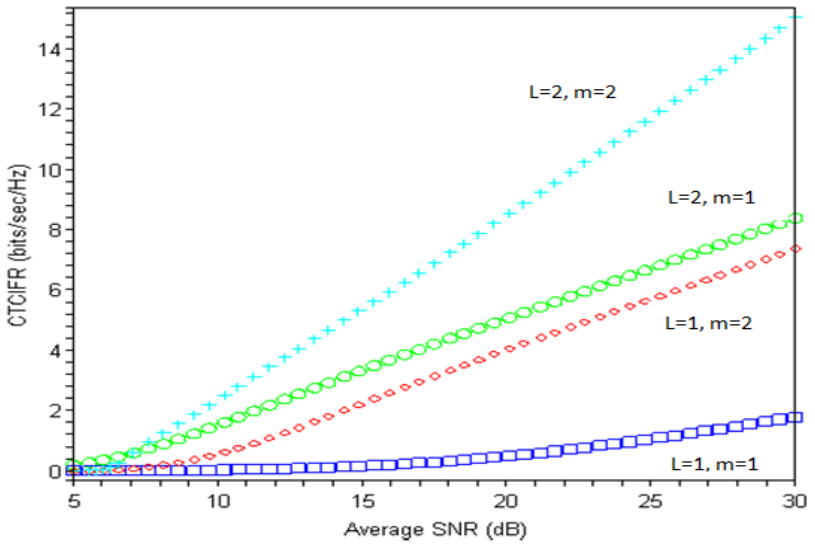

(a)

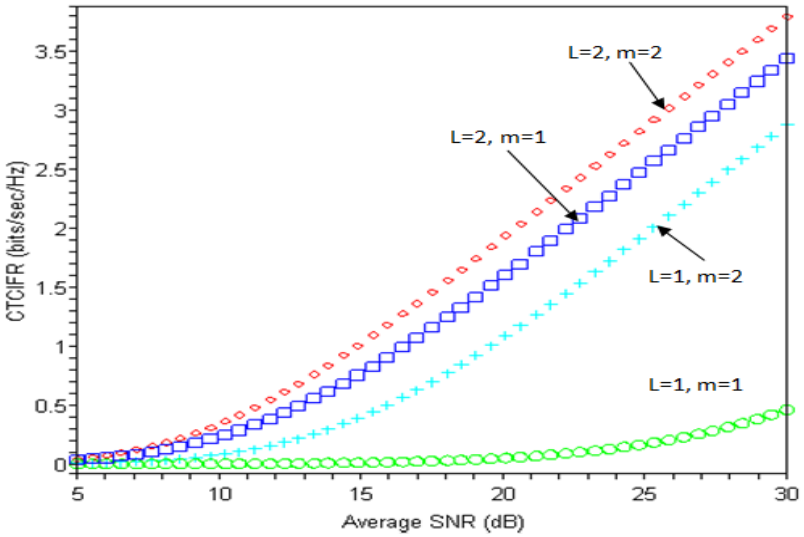

(b)

Fig. 4.2 The response of channel capacity with truncated channel inversion and fixed rate with respect to average SNR for different values of diversity branches L and fading parameter m with chosen values of shadowing parameters for (a) k =75.11 and (b) k=1.0931.

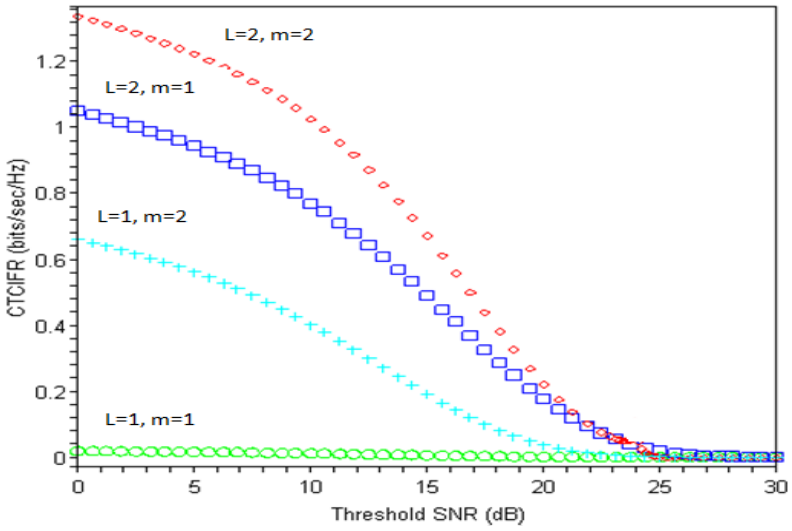

(a)

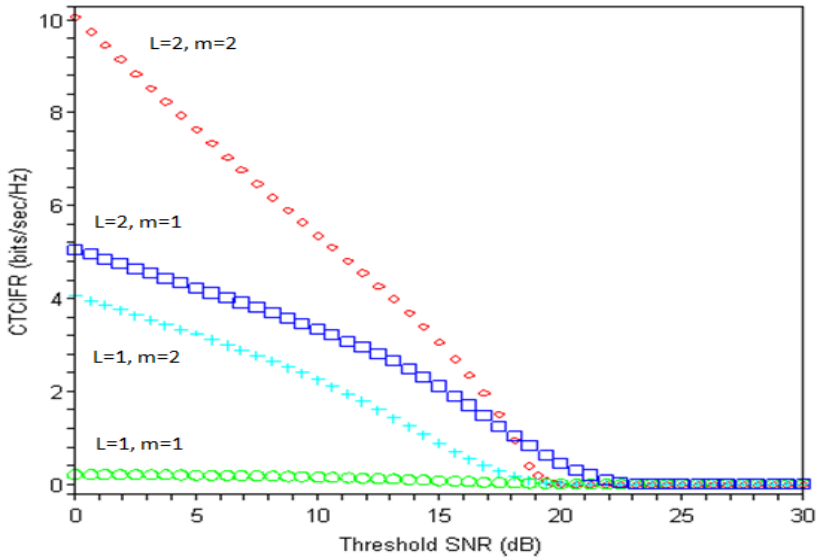

(b)

Fig.4.3 The response of channel capacity with truncated channel inversion and fixed rate with respect to threshold SNR for different values of diversity branches L and fading parameter m with chosen values of shadowing parameters for (a) k=1.0931 and (b) k=75.11.

4.6 Summary

In this chapter, the advantage of employing diversity combining technique at the receiver is provided. The analytical expression for the channel capacity with truncated channel inversion and fixed rate over MRC combining technique is provided and performance analysis is done. The channel capacity is shown to improve with the number of diversity branches and the values of fading and shadowing parameters.

CHAPTER 5

CONCLUSION AND FUTURE SCOPE

5.1 Conclusion

We have presented MMGF based channel capacity analysis for suboptimal adaptation technique for Generalized-K fading channel where the power is adapted in accordance to channel state information with fixed transmission rate which is simple and novel approach. The perfect channel state information is assumed to be available at the transmitter so that it can adapt in accordance to the channel state. We have derived analytical expressions for the channel capacity under channel inversion with fixed rate (C_{CIFR}) and for the truncated channel inversion with fixed rate (C_{TCIFR}), which is valid for arbitrary values of the shaping parameters *k* and *m* and where, *k*-*m* is not an integer. The C_{CIFR} is calculated by using Equation (15), which is similar with [82 eq. 27] and [78 eq. 19]. The expression for channel capacity with truncated channel inversion for fixed rate over Generalized-K faded channel in terms of MMGF is given and performance analysis over that expression is performed.

In addition to this, we have exploited significantly more accurate approximation for practical wireless channels with combined effect of path loss, shadowing and multipath fading. The introduction of DAS has further lead to the improved efficiency of wireless networks due to improved channel capacity and better coverage with reduced transmission energy requirement. A system model of DAS with transparent relaying technique and fixed relay nodes is considered over composite fading environment and numerical analysis is provided. The analytical expressions using numerical approximation has been derived for the outage probability and channel capacity for single node relaying and multiple node relaying techniques for the proposed system model. The simulation results have been shown to validate the performance improvement with the use of DAS, and much closer approximation to practical scenario is provided by

considering the combined effect of various types of fading in a more generalized form. Further, the improvement to this proposed system model can be provided by considering adaptive techniques at the transmitter with the use of channel state information (CSI), which will be reported in future communication.

5.2 Future scope

The channel capacity analysis over Generalized-K fading environment is provided in first section of this dissertation. The adaptive technique has been considered which is being exploited by the use of CSI at the transmitter. The analysis is made under the assumption of perfect CSI that is, the feedback path from the receiver to the transmitter is error free and delay less. However, this assumption is not valid for practical scenarios and therefore, the imperfect CSI can be considered as the extension for this work. Furthermore, the Generalized-K fading channel can be extended to multiple antenna communication system and also the diversity combining techniques other than MRC can be considered for analysis.

The proposed model for DAS can be further extended to regenerative relaying techniques with mobile nodes. The ad hoc distributed communication system is the future of wireless communication system and therefore, the mobile nodes with decode and forward relaying can be proposed in place of the transparent and fixed relay nodes. The configuration of the relay nodes considered can be extended to the series combination to mitigate the path loss effects. The composite fading model proposed with the combination of path loss, shadowing and multipath fading can be further extended to cooperative communication.

APPENDIX

APPENDIX: A

BER analysis over Generalized-K fading channel

PDF based approach: The average probability of error over composite fading channel is given as [70]:

$$P_{avg}(e) = \int_0^{\infty} P(^{e}/_{x})\, f_X(x) dx$$

where, $f_X(x)$ is the probability density function of the signal envelope X [70, Eq. (5)] and $P(^{e}/_{x})$ is the probability of error for BPSK conditioned on fading channel [70, Eq. (9)].

MGF based approach: by using the alternate form of *erfc* function [11], the average BER over Generalized-K fading channel in terms of MGF is given as [78, Eq. (5)]

$$P_{avg}(e) = \frac{1}{\pi} \int_0^{\pi/2} M_{\gamma}\left(\frac{g}{sin^2(\theta)}\right) d\theta$$

where, g is a constant and have different values for different type of modulation schemes such as g=1 for BPSK and g=1/2 for coherent detection of BFSK and g=0.715 for coherent detection of minimum shift keying [78].

The closed form expression for the average BER in terms of MeijerG is given as [78, Eq. (6)]

$$P_{avg}(e) = \frac{(^{\Xi}/_{g})^{\beta+1/2}}{2\sqrt{\pi}\,\Gamma(m)\Gamma(k)}\, G_{2,3}^{2,2}\left[\frac{\Xi}{g}, \quad \begin{matrix} -\beta/2 & (1-\beta)/2 \\ \alpha/2 & -\alpha/2 \quad -(1+\beta)/2 \end{matrix}\right]$$

APPENDIX: B

SIMULATION CODES

1. Source code for channel capacity analysis of truncated channel inversion with fixed rate (C_{TCIFR}) over Generalized-K fading channel:

```
> restart:
> m:=2.0000001: ks:=[1.0931,75.11]: a:=k-m: b:=k+m-1: snr:=15:
> z:=(k*m)/10^(0.1*snr):
ps:=[0.01,1.01,2.01,3.01,4.01,5.01,6.01,7.01,8.01,9.01,10.01]:
> n1:={seq((((10^(0.1*yo))^((b-a+2*p-1)/2)*z^((b-a+2*p+1)/2)*GAMMA((1-
(b-a+2*p))/2))/(p!*GAMMA(p-a+1)*GAMMA(1+((1-(b-a+2*p))/2)))),p=ps)}:
> N1:=convert(n1,`+`):
> n2:={seq((((10^(0.1*yo))^((b+a+2*p-1)/2)*z^((b+a+2*p+1)/2)*GAMMA((1-
(b+a+2*p))/2))/(p!*GAMMA(p+a+1)*GAMMA(1+((1-(b+a+2*p))/2)))),p=ps)}:
> N2:=convert(n2,`+`):
> x:=((Pi*csc(a*Pi))/(GAMMA(m)*GAMMA(k))):
> c:=abs(x*(N1-N2)):
> cc:=evalf(log[2](1+(1/c))):
> me:=MeijerG([[],[1-((b+1)/2)]],[[-(b+1)/2,a/2,-
a/2],[]],(z*(10^(0.1*yo)))):;
> m1:=((z*(10^(0.1*yo)))^((b+1)/2))/(GAMMA(m)*GAMMA(k)):
> po:=m1*me:
> cap:={seq(cc*0.5*po,k=ks)}:
> with(plots):
>
F:=plot(cap,yo=0..30,color=[yellow,green,blue],style=point,symbol=[cros
s,circle,box],labels=["Threshold SNR (dB)","CTCIFR
(bits/sec/Hz)"],labeldirections=[horizontal,vertical]):
> ns:=[1.0000001,2.0000001,5.0000001]: l:=1.0931: ax:=l-n: bx:=l+n-1:
snr:=15:
> zx:=(l*n)/10^(0.1*snr):
ps:=[0.01,1.01,2.01,3.01,4.01,5.01,6.01,7.01,8.01,9.01,10.01]:
> n1x:={seq((((10^(0.1*yo))^((bx-ax+2*p-1)/2)*zx^((bx-
ax+2*p+1)/2)*GAMMA((1-(bx-ax+2*p))/2))/(p!*GAMMA(p-ax+1)*GAMMA(1+((1-
(bx-ax+2*p))/2)))),p=ps)}:
> N1x:=convert(n1x,`+`):
> n2x:={seq((((10^(0.1*yo))^((bx+ax+2*p-
1)/2)*zx^((bx+ax+2*p+1)/2)*GAMMA((1-
(bx+ax+2*p))/2))/(p!*GAMMA(p+ax+1)*GAMMA(1+((1-
(bx+ax+2*p))/2)))),p=ps)}:
> N2x:=convert(n2x,`+`):
> xx:=((Pi*csc(ax*Pi))/(GAMMA(n)*GAMMA(l))):
> cx:=abs(xx*(N1x-N2x)):
> ccx:=evalf(log[2](1+(1/cx))):
> mex:=MeijerG([[],[1-((bx+1)/2)]],[[-(bx+1)/2,ax/2,-
ax/2],[]],(zx*(10^(0.1*yo)))):;
> m1x:=((zx*(10^(0.1*yo)))^((bx+1)/2))/(GAMMA(n)*GAMMA(l)):
> pox:=m1x*mex:
> capx:={seq(ccx*0.5*pox,n=ns)}:
> with(plots):
```

```
>G:=plot(capx,yo=0..30,color=[blue,cyan,red],style=point,symbol=[box,di
amond,point],labels=["Threshold SNR (dB)","CTCIFR
(bits/sec/Hz)"],labeldirections=[horizontal,vertical]):
> display({F,G});
```

2. Source code for outage probability analysis for DAS with N number of relay nodes per cell over composite fading channel:

```
> restart:
> rho:=300:theta:=0: d1:=300: d2:=300: d3:=300: theta1:=(Pi)/2:
theta2:=Pi: theta3:=(3*Pi)/2:beta:=1.9: m:=1: v:=1: mu:=10^(0.1*0):
sigmas:=[10^(0.1*0),10^(0.1*8),10^(0.1*13)]:d0:=20:gamma0:=10^(0.1*10):
a:=0:b:=0:c:=0:
> mu1:=mu+10*log[10]((10^(0.1*snr))*((d0/sqrt((rho^2)+(d1^2)-
2*rho*d1*cos(theta-theta1))))^beta):
> mu2:=mu+10*log[10]((10^(0.1*snr))*((d0/sqrt((rho^2)+(d2^2)-
2*rho*d2*cos(theta-theta2))))^beta):
> mu3:=mu+10*log[10]((10^(0.1*snr))*((d0/sqrt((rho^2)+(d3^2)-
2*rho*d3*cos(theta-theta3))))^beta):
> tn:=[-1.65068,-0.524648,0.524648,1.65068]:
> Hn:=[0.0813128,0.80491,0.80491,0.0813128]:
> for ii from 1 to 4 do
a:=Hn[ii]*GAMMA(m,m*(((gamma0/10^((sqrt(2)*sigma*tn[ii]+mu1)/10)))^v))+
a
od:
> for ii from 1 to 4 do
b:=Hn[ii]*GAMMA(m,m*(((gamma0/10^((sqrt(2)*sigma*tn[ii]+mu2)/10)))^v))+
b
od:
> for ii from 1 to 4 do
c:=Hn[ii]*GAMMA(m,m*(((gamma0/10^((sqrt(2)*sigma*tn[ii]+mu3)/10)))^v))+
c
od:
> pout:={seq((1-(a/(sqrt(Pi)*GAMMA(m))))*(1-
(b/(sqrt(Pi)*GAMMA(m))))*(1-(c/(sqrt(Pi)*GAMMA(m)))),sigma=sigmas)}:
> with(plots):
> plot(pout,snr=0..50,labels=["Average SNR
(dB)","Pout"],color=[red,green,blue],style=point,symbol=[point],labeldi
rections=[horizontal,vertical]);
```

3. Source code for channel capacity analysis for DAS with N number of relay nodes per cell over composite fading channel:

```
> restart:
> rho:=300:theta:=0: d1:=300: d2:=300: d3:=300: theta1:=(Pi)/2:
theta2:=Pi: theta3:=(3*Pi)/2:beta:=2: m:=1: mu:=10^(0.1*0):
sigma:=10^(0.1*8):d0:=20:a:=0:b:=0:c:=0:ks:=[1]:
> mu1:=mu+10*log[10]((10^(0.1*snr))*((d0/sqrt((rho^2)+(d1^2)-
2*rho*d1*cos(theta-theta1))))^beta):
> mu2:=mu+10*log[10]((10^(0.1*snr))*((d0/sqrt((rho^2)+(d2^2)-
2*rho*d2*cos(theta-theta2))))^beta):
```

```
> mu3:=mu+10*log[10]((10^(0.1*snr))*((d0/sqrt((rho^2)+(d3^2)-
2*rho*d3*cos(theta-theta3))))^beta):
> tn:=[-1.65068,-0.524648,0.524648,1.65068]:
> Hn:=[0.0813128,0.80491,0.80491,0.0813128]:
> for ii from 1 to 4 do
a:=((m^(m-
k))/sqrt(Pi))*Hn[ii]*exp(m/10^((sqrt(2)*sigma*tn[ii]+mu1)/10))*((10^((s
qrt(2)*sigma*tn[ii]+mu1)/10))^(k-m))*GAMMA(k-
m,(m/10^((sqrt(2)*sigma*tn[ii]+mu1)/10)))+a
od: a1:={seq(a,k=ks)}:a2:=convert(a1,`+`):
> for ii from 1 to 4 do
b:=((m^(m-
k))/sqrt(Pi))*Hn[ii]*exp(m/10^((sqrt(2)*sigma*tn[ii]+mu2)/10))*((10^((s
qrt(2)*sigma*tn[ii]+mu2)/10))^(k-m))*GAMMA(k-
m,(m/10^((sqrt(2)*sigma*tn[ii]+mu2)/10)))+b
od:b1:={seq(b,k=ks)}:b2:=convert(b1,`+`):
> for ii from 1 to 4 do
c:=((m^(m-
k))/sqrt(Pi))*Hn[ii]*exp(m/10^((sqrt(2)*sigma*tn[ii]+mu3)/10))*((10^((s
qrt(2)*sigma*tn[ii]+mu3)/10))^(k-m))*GAMMA(k-
m,(m/10^((sqrt(2)*sigma*tn[ii]+mu3)/10)))+c
od:c1:={seq(c,k=ks)}:c2:=convert(c1,`+`):
> cap:=a2:
> with(plots):
>
F:=plot(cap,snr=0..40,color=[red],style=point,symbol=[cross],labels=["A
verage SNR
(dB)","Capacity(bits/sec/Hz)"],labeldirections=[horizontal,vertical]):
> n:=5: ps:=[1,2,3,4,5]: x:=0: y:=0: z:=0:
> for ii from 1 to 4 do
x:=((n^(n-
p))/sqrt(Pi))*Hn[ii]*exp(n/10^((sqrt(2)*sigma*tn[ii]+mu1)/10))*((10^((s
qrt(2)*sigma*tn[ii]+mu1)/10))^(p-n))*GAMMA(p-
n,(n/10^((sqrt(2)*sigma*tn[ii]+mu1)/10)))+x
od: x1:={seq(x,p=ps)}:x2:=convert(x1,`+`):
> for ii from 1 to 4 do
y:=((n^(n-
p))/sqrt(Pi))*Hn[ii]*exp(n/10^((sqrt(2)*sigma*tn[ii]+mu2)/10))*((10^((s
qrt(2)*sigma*tn[ii]+mu2)/10))^(p-n))*GAMMA(p-
n,(n/10^((sqrt(2)*sigma*tn[ii]+mu2)/10)))+y
od:y1:={seq(y,p=ps)}:y2:=convert(y1,`+`):
> for ii from 1 to 4 do
z:=((n^(n-
p))/sqrt(Pi))*Hn[ii]*exp(n/10^((sqrt(2)*sigma*tn[ii]+mu3)/10))*((10^((s
qrt(2)*sigma*tn[ii]+mu3)/10))^(p-n))*GAMMA(p-
n,(n/10^((sqrt(2)*sigma*tn[ii]+mu3)/10)))+z
od:z1:={seq(z,p=ps)}:z2:=convert(z1,`+`):
> cap1:=x2:
> with(plots):
>
G:=plot(cap1,snr=0..40,color=[blue],style=point,symbol=[box],labels=["A
verage SNR
(dB)","Capacity(bits/sec/Hz)"],labeldirections=[horizontal,vertical]):
> display({F,G});
```

REFERENCES

[1] S. Haykin, “Communication Systems”, Fourth Edition, John Wiley & Sons, Inc., Singapore, 2001.

[2] A. Goldsmith, “Wireless Communications”, 1st edition, Stanford University, Cambridge University Press, New York, 2005.

[3] T. S. Rappaport, “Wireless Communications Principles and Practice”, Second edition, Pearson Education Inc., 2002.

[4] A. Arsal, “A study on wireless channel models: Simulation of fading, shadowing and further applications”, MS thesis, Graduate school of Engineering and sciences of Izmir Institute of technology, August 2008.

[5] P.M. Shankar, “Statistical models for fading and Shadowed fading channels in Wireless Systems: A Pedagogical Perspective”, Wireless personal communications, vol. 60, no. 2, pp. 191-213, 2011.

[6] M.S. Alouini, “Adaptive and diversity techniques for wireless digital communication over fading channels”, Doctor of philosophy thesis, California Institute of technology, Pasadena, California, 1998.

[7] M.K. Simon and M.S. Alouini, “Digital Communication over Fading Channel: A Unified Approach to Performance Analysis”, John Wiley and Sons, Inc., New York, 2000.

[8] L. Rayleigh, “On the resultant of a large number of vibrations of the same pitch and of arbitrary phase”, Philosophical Magazine, vol. 27, pp. 460-469, June 1889.

[9] H.W. Nylund, “Characteristics of small-area signal fading on mobile circuits in the 150 MHz band”, IEEE Transactions on Vehicular Technology, vol. 17, no. 1, pp. 24- 30, 1968.

[10] Y. Okumara, E. Ohmori, T. Kawano and K. Fukuda, “Field strength and its variability in VHF and UHF land mobile radio services”, Review of the Electrical Communication Laboratory, vol. 16, no. 9-10, pp. 825-873, 1968.

[11] M.K. Simon and M.S. Alouini, “Digital Communication over Fading Channels”, 2nd edition, Wiley, New York, 2005.

[12] H.B. James and P.I. Wells, “Some tropospheric scatter propagation measurements near the radio-horizon”, Proc. IEEE of the IRE, vol. 43, no. 10, pp. 1336-1340, October 1955.

[13] R. S. Hoyt, “Probability functions for the modulus and angle of the normal complex variate”, Bell Systems Technical Journal, vol. 26, no. 4, pp. 318 -359, 1947.

[14] I.S. Gradshteyn, & I.M. Ryzhik, “Table of integrals, series, and products” ,7th edition, Academic Press, New York, 2007.

[15] B. Chytil, “The distribution of amplitude scintillation and the conversion of scintillation indices”, J. of Atmospheric and Terrestrial Physics, vol. 29, no. 9, pp. 1175 -1177, 1967.

[16] A. Mehrnia and H. Hashemi, “Mobile satellite propagation channel part II- a new model and its performance”, Proc. IEEE on Vehicular Technology Conference, Amsterdam, Netherland, vol. 5, pp. 2780-2784, 1999.

[17] R. J. C. Bultitude, S. A. Mahmoud, and W. A. Sullivan, “A comparison of indoor radio propagation characteristics at 910 MHz and 1.75 GHz”, IEEE J. on Selected Areas in Communications, vol. 7, no. 1, pp. 20-30, 1989.

[18] S.O. Rice, “Statistical properties of a sine wave plus random noise”, Bell System Technical Journal, vol. 27, no. 1, pp. 109- 157, 1948.

[19] M. Nakagami, “The m-distribution—A general formula of intensity distribution of rapid fading”, Statistical Methods in Radio Wave Propagation, vol 6a, no. 7-36, pp. 3-36, 1960.

[20] S.R. Panic, M. Stefanovic, J. Anastasov and P. Spalevic,“Fading and Interference Mitigation in Wireless Communications”, CRC Press, Taylor & Francis Group, Boca Raton, 2014.

[21] P. Papoulis,"Probability, random variables and Stochastic Processes", Fourth Edition, McGraw-Hill Companies, New York, 2002.

[22] G. Tzeremes and C.G. Christodoulou," Use of Weibull distribution for describing outdoor multipath fading", Proc. IEEE of Antennas and Propagation Society International Symposium, San Antonio, Texas, vol. 1, pp. 232-235, 2002.

[23] H. Hashemi, "The indoor radio propagation channel", Proc. IEEE, vol. 81, no. 7, pp. 943-968, 1993.

[24] F. Babich and G. Lombardi, "Statistical analysis and characterization of the indoor propagation channel", IEEE Transactions on Communications, vol. 48, no. 3, pp. 455-464, 2000.

[25] N.C. Sagias and G.K. Karagiannidis, "Gaussian class multivariate Weibull distributions: Theory and applications in fading channels", IEEE Transactions on Information Theory, vol. 51, no. 10, pp. 3608-3619, 2005.

[26] J.Y. Wang, J.B. Wang, X.Y. Dang, M. Lin, Y. Jiao and M. Chen, "System capacity analysis of downlink distributed antenna system over composite channels", IEEE International Conference on Communication and Technology, Nanjing, pp. 1076-1079, 11-14 November 2010.

[27] X.H. You, D.M. Wang, B. Sheng, X.Q. Gao, X.S. Zhao and M. Chen, "Cooperative distributed antenna systems for mobile communications", IEEE Wireless Communications, vol. 17, no. 3, pp. 35-43, 2010.

[28] J.Y. wang, J.B. Wang and M. Chen, "System capacity analysis and antenna placement optimization for downlink transmission in distributed antenna systems", Wireless personal Communication, vol. 71, no.1, pp. 531- 554, 2012.

[29] M. Dohler and Y. Li, "Cooperative Communications: Hardware, Channel and PHY", First edition, Wiley, Chichester, 2010.

[30] B. Talha and M. Patzold, “Channel models for mobile-to-mobile cooperative communication systems: A state of the art review”, IEEE Vehicular Technology Magazine, vol. 6, no. 2, pp. 33-43, June 2011.

[31] J. N. Laneman, D. N. C. Tse, and G. W. Wornell, “Cooperative diversity in wireless networks: Efficient protocols and outage behavior,” IEEE Transactions on Information Theory, vol. 50, no. 12, pp. 3062–3080, Dec. 2004.

[32] D. Soldani and S. Dixit, “Wireless relays for broadband access”, IEEE Communications Magazine, vol. 46, no. 3, pp. 58-66, March 2008.

[33] C. X. Wang, X. Hong, X. Ge, X. Cheng, G. Zhang and J. Thompson, “Cooperative MIMO channel models: A Survey”, IEEE Communications Magazine, vol. 48, no. 2, pp. 80-87, February 2010.

[34] D. A. Palmer and A. J. Motely, “Controlled radio coverage within buildings”, British Telecommuinication Technolology Journal, vol. 4, pp. 55–57, Oct. 1986.

[35] A. Saleh, A. Rustako, and R. Roman, “Distributed antennas for indoor radio communications”, IEEE Transactions on Communications, vol. 35, no. 12, pp. 1245–1251, Dec. 1987.

[36] A. Salmasi and K. Gilhousen, “On the system design aspects of code division multiple access (CDMA) applied to digital cellular and personal communications networks”, Proc. IEEE on Vehicular Technology Conference (VTC), pp. 57-62, 19-22 May 1991.

[37] H. Yanikomeroglu and E. S. Sousa, “CDMA distributed antenna system for indoor wireless communications”, Proc. IEEE on 2nd International Conference on Universal Personal Communications (ICUPC), Ottawa, vol. 2, 12-15 October 1993.

[38] H. Xia, A. Herrera, S. Kim, and F. Rico, “A CDMA-distributed antenna system for in-building personal communications services”, IEEE J. on Selected Areas in Communications, vol. 14, no. 4, pp. 644–650, May 1996.

[39] H. Yanikomeroglu and E. Sousa, “Power control and number of antenna elements in CDMA distributed antenna systems”, proc. IEEE of International Conference on Communications (ICC), Atlanta, vol. 2, 7-11 June 1998.

[40] A. Obaid and H. Yanikomeroglu, “Reverse-link power control in CDMA distributed antenna systems”, Proceedings of IEEE Wireless Communications and Networking Conference (WCNC*)*, Chicago, vol. 2, pp. 608-612, 23- 28 September 2000.

[41] L. Dai, S. Zhou, and Y. Yao, “Capacity analysis in CDMA distributed antenna systems”, IEEE Transactions on Wireless Communications, vol. 4, no. 6, pp. 2613–2620, Nov. 2005.

[42] H. Yanikomeroglu and E. S. Sousa, “CDMA sectorized distributed antenna system”, IEEE 5th International Symposium on Spread Spectrum Techniques and Applications Proceedings, Sun City, vol. 3, pp. 792- 797, 2- 4 September 1998.

[43] H. Yanikomeroglu and E. Sousa, “SIR-balanced macro power control for the reverse link of CDMA sectorized distributed antenna system”, Proc. IEEE of International Symposium on Personal, Indoor and Mobile Radio Communications (PIMRC), Boston, vol. 2, pp. 915- 920, 8- 11 September 1998.

[44] S.A. Ahmadi, “Composite Fading Channel Modeling and Information Capacity of Distributed Antenna Architectures in Cellular Networks”, Doctor of Philosophy Thesis, The Ottawa-Carleton Institute for Electrical and Computer Engineering (OCIECE), Department of Systems and Computer Engineering Carleton University, Ottawa, Ontario, Canada , July 2010.

[45] H. Hu, Y. Zhang, and J. Luo, “Distributed Antenna Systems: Open Architecture for Future Wireless Communications”, CRC: CRC Press, 2007.

[46] P. Marsch and G. Fettweis, “A framework for optimizing the uplink performance of distributed antenna systems under a constrained backhaul”, Proc. IEEE of International Conference on Communications (ICC), Glasgow, pp. 975- 979, 24- 28 June 2007.

[47] S.A. Ahmadi and H. Yanikomeroglu, "The ergodic and outage capacities of distributed antenna systems in generalized-K fading channels", IEEE 21st International Symposium on Personal Indoor and Mobile Radio Communications, Istanbul, pp. 662-666, 26-30 September 2010.

[48] W. Roh and A. Paulraj, "MIMO channel capacity for the distributed antenna systems", Proc. IEEE of Vehicular Technology Conference, Piscataway, vol. 2, pp. 706-709, 2002.

[49] L. Dai, S. Zhou and Y. Yao, "Capacity analysis in CDMA distributed antenna systems", IEEE Transactions on Wireless Communication, vol. 4, no. 6, pp. 2613-2620, 2005.

[50] H.R. Zhuang, L. Dai and L. Xiao, "Spectral efficiency of distributed antenna system with random antenna layout", IEEE Electronics Letters, vol. 39, no. 6, pp. 495–496, 2003.

[51] H. Zhu, "Performance comparison between distributed antenna and microcellular systems", IEEE J. on Selected Areas in Communications, vol. 29, no. 6, pp. 1151-1163, 2011.

[52] V. Nikolopolous, M. Fiacco, S. Stavrou and S.R. Saunders, "Narrowband fading analysis of indoor distributed antenna systems", IEEE Antennas Wireless Propagation Letter, vol. 2, no.1, pp. 89-92, 2003.

[53] M. Matthaiou, N. Chatzidiamantis and G. Karagiannidis, "A new lower bound on the ergodic capacity of distributed MIMO systems", IEEE Signal Processing Letter, vol. 18, no. 4, pp. 227-230, 2011.

[54] H.M. Chen, J.B. Wang and M.Chen, "Outage capacity study of the distributed MIMO system with antenna cooperation", Wireless Personal Communication", vol. 54, no. 4, pp. 599-605, 2011.

[55] J. Zhang and J.G. Andrews, "Distributed antenna system with randomness", IEEE Transactions on Wireless Communication, vol. 7, no. 9, pp. 3636-3646, 2008.

[56] H.M. Chen, J.B. Wang and M.Chen, "Outage performance of distributed antenna systems over shadowed Nakagami-m fading channels", European Transactions on Telecommunication, vol. 20, no. 5, pp. 531-535, 2009.

[57] C.H.M. de Lima, M. Bennis and M. Latva-aho, "Statistical analysis of self-organizing heterogeneous networks with biased cell association and interference avoidance", IEEE Transactions on Vehicular Technology, vol. 62, no. 5, pp. 1950-1961, 2013.

[58] E.W. Stacy, "A generalization of the gamma distribution", The Annals of Mathematical Statistics, vol. 33, no. 3, pp. 1187-1192, 1962.

[59] M.K. Simon and M.S. Alouini, "A unified approach to performance analysis of digital communication over Generalized fading channels", Proc. IEEE, vol. 86, no. 9, pp. 1860-1877, September 1998.

[60] D. Shen, A. Lu, Y. Cui, F. Kuang, X. Zhang, K. Wu and J. Yao, "On the channel capacity of MIMO Rayleigh-Lognormal fading channel", IEEE International Conference on Microwave and Millimeter Wave Technology, Chengdu, pp. 156-159, 8-11 May 2010.

[61] A.M. Mitic and M.M. Jakovljevic, "Second-order statistics in Weibull-Lognormal fading channels", IEEE 8th International Conference on Telecommunications in Modern Satellite, Cables and Broadcasting Services (TELSIKS), Serbia, pp. 529-532, 26-28 September 2007.

[62] P. Karadimas and S.A. Kotsoplolous, "The Weibull–Lognormal Fading Channel: Analysis, Simulation, and Validation", IEEE Transactions on Vehicular Technology, vol. 58, no. 7, pp. 3808- 3813, 2009.

[63] A.H. Gaber, M.H. Ismail and H.M. Mourad, "Outage probability analysis of cooperative diversity networks over Weibull and Weibull-Lognormal channels", Wireless Personal Communications, vol. 70, no. 2, pp. 695-708, May 2013.

[64] T.T. Tjhung and C.C. Chai, "Fade statistics in Nakagami-lognormal channels", IEEE Transactions on Communications, vol. 47, no. 12, pp. 1769-1772, December 1999.

[65] P. Xu, X. Zhou and D. Hu, "Performance evaluations of adaptive modulation over composite Nakagami-lognormal fading channels", IEEE 15th Asia-Pacific Conference on Communications, Shanghai, pp. 467-470, 8-10 October 2009.

[66] A. Abdi, and M.K. Kaveh, "K distribution: An approximate substitute for Rayleigh-lognormal distribution in fading-shadowing wireless channels", Electronics Letter, vol. 34, no. 9, pp. 851–852, 1998.

[67] A. Abdi, and M.K. Kaveh, "Comparison of DPSK and MSK bit error rates for K and Rayleigh-lognormal fading distributions", IEEE Communications Letters, vol. 4, no.4, pp. 122-124, April 2000.

[68] D.R. Iskander, A.M. Zoubir, and B. Boashash, "A method for estimating the parameters of the K distribution", IEEE Transactions on Signal Processing, vol. 47, no. 4, pp. 1147-1151, April 1999.

[69] P. Theofilakos, A.G. Kanatas, and G.P. Efthymoglou, "Performance of generalized selection combining receivers in k fading channels", IEEE Communications Letters, vol. 12, no. 11, pp. 816-818, November 2008.

[70] P.M. Shankar, "Error rates in generalized shadowed fading channels", Wireless personal communications, vol. 28, no.3, pp. 233-238, 2004.

[71] P.S. Bithas, N.C. Sagias, P.T. Mathiopoulos, G.K. Karagiannidis and A.A. Rontogiannis, "On the Performance Analysis of Digital Communications over Generalized-*K* Fading Channels", IEEE Communication Letters, vol. 10, no. 5, May 2006.

[72] M.S. Alouini, A. Abdi, and M. Kaveh, "Sum of gamma variates and performance of wireless communication systems over Nakagami-fading channels", IEEE

Transactions on Vehicular Technology, vol. 50, no. 6, pp. 1471–1480, November 2001.

[73] W. Lee, “Estimate of channel capacity in Rayleigh fading environment”, IEEE Transactions on Vehicular Technology, vol. 39, no. 3, pp. 187–189, August 1990.

[74] C. G. Gunther, “Comments on ‘Estimate of channel capacity in Rayleigh fading environment’”, IEEE Transactions on Vehicular Technology, vol. 45, no. 2, pp. 401- 403, May 1996.

[75] Q. T. Zhang and D. P. Liu, “Simple capacity formulas for correlated SIMO Nakagami channels”, Proc. IEEE of Vehicular Technology Conference, vol. 1, pp. 554- 556, April 2003.

[76] N. C. Sagias, G. S. Tombras, and G. K. Karagiannidis, “New results for the Shannon channel capacity in generalized fading channels”, IEEE Communications Letter, vol. 9, no. 2, pp. 97–99, Feb. 2005.

[77] K. A. Hamdi, “Capacity of MRC on correlated Rician fading channels”, IEEE Transactions on Communications, vol. 56, no. 5, pp. 708–711, May 2008.

[78] V.K. Dwivedi and G. Singh, “Moment Generating Function based performance analysis of Maximal Ratio Combining Diversity receivers in the generalized k-fading channels”, Wireless Personal Communications, vol. 77, no. 3, pp. 1959-1975, February 2014.

[79] I.M. Kostic, “Composite phase PDF in Gamma Shadowed Nakagami fading channel”, Wireless personal communications, vol 41, no. 4, pp. 465-469, 2007.

[80] G.P. Efthymoglou, “On the performance analysis of digital modulations in Generalized-k fading channels”, Wireless Personal Communications, vol. 65, no. 3, pp. 643–651, 2012.

[81] Laourine, A.,Alouini, M.S., Affes, S. and St´ephenne, A., “On the capacity of Generalized-k fading channels”, IEEE Transactions on Wireless Communications, vol. 7, no. 7, pp. 2441-2445, July 2008.

[82] G.P. Efthymoglou, N.Y. Ermolova and V.A. Aalo, "Channel capacity and average error rates in generalized-K fading channels", IET Communications, vol. 4, no. 11, pp. 1364- 1372, 2010.

[83] M.D. Renzo, F. Graziosi and F. Santucci, "Channel capacity over generalized fading channels: A novel MGF-based approach for performance analysis and design of wireless communication systems", IEEE Transactions on Vehicular Technology, vol. 59, no.1, pp. 127-149, January 2010.

[84] J. Cao, L.L.Yang and Z. Zhong, "Performance of multihop wireless links over generalized-K fading channels", 72nd IEEE Vehicular Technology Conference Fall, Ottawa,ON, pp. 1-5, 6-9 September 2010.

[85] F. Yilmaz and M.S. Alouini, "A unified MGF-based capacity analysis of diversity combiners over generalized fading channels", IEEE Transactions on Communications, vol. 10, no. 20, pp. 1-26, December 2010.

[86] C.E. Shannon, "A mathematical theory of communication", Bell Systems Technology Journal, vol. 27, pp. 379-423, July 1948.

[87] A.J. Goldsmith and P.P. Varaiya, "Capacity of fading channels with channel side information", IEEE Transactions on Information Theory, vol. 43, no. 6, pp. 1986-1992, November 1997.

[88] S. Pandit and G. Singh, "Channel capacity in fading environment with CSI and interference power constraints for cognitive radio communication system", Wireless Networks, (Online) Nov. 2014, DOI 10.1007/s11276-014-0849-0.

[89] V. K. Dwivedi and G. Singh, "Marginal moment generating function based analysis of channel capacity over correlated Nakagami-m fading with maximal-ratio combining diversity", Progress In Electromagnetics Research, vol. 41, pp. 333-356, 2012.

[90] V. K. Dwivedi and G. Singh, "A novel moment generating function based performance analysis over correlated Nakagami-m fading", Journal of Computational Electronics, vol. 10, no. 4, pp. 373-381, December 2011.

[91] Y.C. Ko, M.S. Alouini, and M. K. Simon, "Outage probability of diversity systems over generalized fading channels", IEEE Transactions on Communications, vol. 48, no. 11, pp. 1783–1787, November 2000.

[92] A. Annamalai, C. Tellambura, and V. K. Bhargava, "Simple and accurate methods for outage analysis in cellular mobile radio systems — a unified approach", IEEE Transactions on Communications, vol. 49, no. 2, pp. 303–316, February 2001.

[93] V. V. Veeravalli, "On performance analysis for signaling on correlated fading channels", IEEE Transactions on Communications, vol. 49, no. 11, pp. 1879-1883, November 2001.

[94] M.S. Alouini and A. Goldsmith, "A unified approach for calculating error rates of linearly modulated signals over generalized fading channels", IEEE Transactions on Communications, vol. 47, no. 92, pp. 1324-1334, September 1999.

[95] The Wolfram Function Site, 2008, available at http://functions.wolfram.com

[96] A.P. Prudnikov, Y.A. Brychkov and O.I. Marichev, "Integrals and Series: More Special Functions", vol. 3, Gordon and Breach Science, 1990.

[97] R. Schoenen, W. Zirwas, and B. H. Walke, "Capacity and coverage analysis of a 3GPP-LTE multihop deployment scenario", Proc. IEEE International Conference on Communications (ICC'08) Workshops, Beijing, China, pp. 31-36, 18-23 May 2008.

[98] A. Bou Saleh, S. Redana, Jyri Hämäläinen, and B. Raaf, "On the coverage extension and capacity enhancement of in-band relay deployments in LTE-Advanced networks", J. of Electrical and Computer Engineering, no. 4, pp. 1–12, 2010.

[99] O¨. Bulakci, S. Redana, B. Raaf, and Jyri Hämäläinen, “Impact of power control optimization on the system performance of relay based LTE-Advanced heterogeneous networks”, J. of Communications and Networks, vol. 13, no. 4, pp. 345–359, August 2011.

[100] Ömer Bulakci, A. Awada, A. Bou Saleh, S. Redana, and Jyri Hämäläinen, “Automated uplink power control optimization in LTE-Advanced relay networks”, EURASIP J. on Wireless Communications and Networking, no. 8, pp. 1–19, January 2013.

[101] Ömer Bulakci, Jyri Hämäläinen, Egon Schulz, “Practical coarse relay site planning: Performance analysis over composite fading/shadowing channels”, International J. of Wireless Information Networks, vol. 21, no. 4, pp. 249-261, December 2014.

[102] W. Feng, Y. Li, S. Zhou, J. Wang and M. Xia, “Downlink capacity of distributed antenna systems in a multi-cell environment”, Proceedings IEEE Wireless Communications and Networking Conference, Budapest, pp. 1-5, 5-8 April 2009.

[103] J. Cai, X. Zhao, J. Wang and M. Gu, “Probabilistic analysis of system outage in distributed antenna systems with composite channels”, EURASIP J. on Wireless Communications and Networking, vol. 147, no.1, pp. 1- 10, 2013.

[104] J. Jung, S.R. Lee, H. Park, S. Lee and I. Lee, “Capacity and error probability analysis of diversity reception schemes over generalized-K fading channels using a mixture gamma distribution”, IEEE Transactions on Wireless Communications, vol. 13, no. 9, pp. 4721-4730, September 2014.